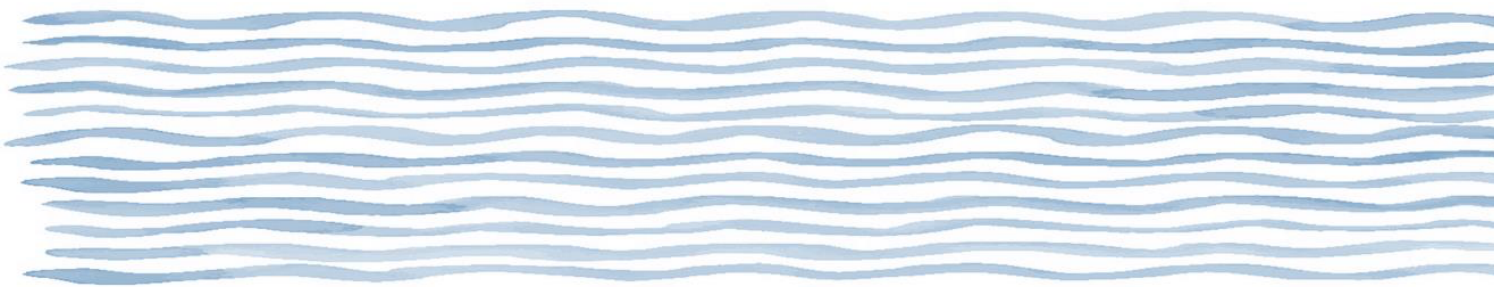**ETH**

Eidgenössische Technische Hochschule Zürich
Swiss Federal Institute of Technology Zurich

SOIL MOISTURE AND EVAPOTRANSPIRATION

M. HIRSCHI, E.L. DAVIN, C. SCHWINGSHACKL, R. WARTENBURGER, R. MEIER, L. GUDMUNDSSON AND S.I. SENEVIRATNE

Impressum

Zusammenfassung

Der vorliegende Bericht "Soil moisture and evapotranspiration" präsentiert eine Literaturübersicht zum aktuellen Forschungsstand und die Resultate aus dem Hydro-CH2018 Forschungsprojekt "Wasserbilanz und Trockenheit", welches die CH2018 Szenarien und deren Unsicherheit hinsichtlich der prognostizierten Änderungen der Verdunstung, der Bodenfeuchte und verschiedener Wasserbilanzindikatoren untersucht hat.

Bodenfeuchte ist definiert als das Wasser, welches in der ungesättigten Zone des Bodens vorliegt. Verdunstung (Evapotranspiration) ist der Fluss von Wasser, welcher von der Landoberfläche und den Ozeanen zurück in die Atmosphäre gelangt. Sowohl Bodenfeuchte als auch Verdunstung sind Schlüsselelemente des Wasser- und Energiekreislaufs und des Kohlestoffzyklus. Bodenfeuchte beeinflusst die Verdunstung durch die Partitionierung der verfügbaren Energie an der Landoberfläche in die sensiblen und latenten Wärmeflüsse. Bodenfeuchte steht den Pflanzen als Wasser zur Verfügung und stellt damit die Hauptwasserquelle für die meisten Ökosysteme dar. Auch beeinflusst die Bodenfeuchte die Abflussbildung und die Grundwasserneubildung.

Das Klimasystem wird durch Bodenfeuchte insbesondere in Regionen beeinflusst, in welchen die Verdunstung wasserlimitiert ist. Mit abnehmender Bodenfeuchte wird verbleibendes Wasser im Boden für die Pflanzen schwerer zugänglich. Deshalb reduziert sich einerseits der Anteil der verfügbaren Energie, welche in den latenten Wärmefluss (und damit Verdunstung) überführt wird. Anderseits erhöht sich dadurch der sensible Wärmefluss, was zu steigenden Lufttemperaturen und Rückkopplungen mit Niederschlag führt.

Für den Sommer und eine starke Erwärmung prognostizieren die CH2018 Szenarien in der Schweiz bis zum Ende des Jahrhunderts eine Reduktion von Regentagen und damit verbunden eine Tendenz für längere Trockenperioden. Die mit der Erwärmung verbundene zusätzliche Verdunstung führt dabei zu einer verstärkten Austrocknung der Böden. Dementsprechend zeigen die untersuchten Dürre- und Wasserbilanzindikatoren bezüglich der globalen Mitteltemperatur für den Alpenraum eine Tendenz zu verstärkter Trockenheit.

Der Umfang der Zunahme der Sommertrockenheit in der Schweiz ist mit grösseren Unsicherheiten behaftet, da die Schweiz in einer Übergangszone zwischen Südeuropa, wo eine starke Zunahme des Dürrerisikos prognostiziert wird, und Nordeuropa, wo mit feuchteren Wintern gerechnet wird, liegt. Die Evaluation der CH2018 Szenarien zeigt, dass die simulierten Dürre- und Wasserbilanzindikatoren im Mittel relativ gut mit den beobachtungsbasierten Indikatoren übereinstimmen. Hingegen trägt die Repräsentation von Prozessen in den regionalen Klimamodellen zur Unsicherheit in den CH2018 Szenarien bei. Namentlich die Berücksichtigung des im Projekt untersuchten pflanzenphysiologische CO_2 Effekts auf die Stomata-Schliessung führt zu einer Reduktion der Verdunstung in Zentral- und Nordeuropa und damit verbunden zu einer Rückkopplung auf die zukünftige Entwicklung der Temperatur und signifikant höheren Temperaturextremen.

Der vom Klimawandel getriebene Bewässerungsbedarf für die Schweiz verdoppelt sich gemäss Modellrechnungen bis Ende des Jahrhunderts. Dieses Signal wird vor allem durch das Tessin, das untere Wallis und die Region Basel dominiert. Die daraus resultierenden Rückkopplungen auf den Wasserkreislauf und die untersuchten Dürre- und Wasserbilanzindikatoren sind jedoch klein und primär in Südeuropa sichtbar.

Résumé

Le présent rapport "Soil moisture and evapotranspiration" présente un tour d'horizon de la littérature scientifique sur l'état actuel de la recherche, ainsi que les résultats du projet de recherche Hydro-CH2018 "Bilan hydrique et sécheresse", qui a étudié les scénarios CH2018 et leurs incertitudes au regard des changements prévus en matière d'évapotranspiration, d'humidité du sol et de différents indicateurs du bilan hydrique.

L'humidité du sol est définie comme l'eau présente dans la zone non saturée du sol. L'évapotranspiration est le flux d'eau de la surface terrestre et des océans qui retourne dans l'atmosphère. Tant l'humidité du sol que l'évapotranspiration sont des éléments clés du cycle de l'eau et de l'énergie et du cycle du carbone. L'humidité du sol influence l'évaporation en répartissant l'énergie disponible à la surface terrestre en flux de chaleur sensible et latente. L'humidité du sol est disponible pour les plantes sous forme d'eau et représente donc la principale source d'eau pour la plupart des écosystèmes. L'humidité du sol influence également la formation du ruissellement et la régénération des nappes phréatiques.

Le système climatique est influencé par l'humidité du sol, en particulier dans les régions où l'évaporation est limitée par la disponibilité en eau. Lorsque l'humidité du sol diminue, l'eau qui reste dans le sol devient plus difficile d'accès pour les plantes. Par conséquent, d'une part, sur toute l'énergie disponible, la proportion d'énergie convertie en flux de chaleur latente (et donc en évaporation) est réduite. D'autre part, le flux de chaleur sensible augmente, ce qui entraîne une hausse des températures de l'air et une répercussion sur les précipitations.

Pour l'été et un fort réchauffement, les scénarios CH2018 prévoient une réduction du nombre de jours de pluie en Suisse d'ici la fin du siècle, associée à une tendance à de plus longues périodes sèches. L'évaporation supplémentaire associée au réchauffement entraînera un dessèchement accru des sols. En conséquence, les indicateurs de sécheresse et de bilan hydrique examinés en rapport avec la température moyenne mondiale montrent une tendance à l'augmentation de la sécheresse dans la région alpine.

L'ampleur de l'augmentation de la sécheresse estivale en Suisse est sujette à une grande incertitude, car la Suisse est située dans une zone de transition entre l'Europe du Sud, où l'on prévoit une forte augmentation du risque de sécheresse, et l'Europe du Nord, où des hivers plus humides sont attendus. L'évaluation des scénarios CH2018 montre qu'en règle générale, les simulations des indicateurs de sécheresse et de bilan hydrique correspondent relativement bien aux indicateurs basés sur l'observation. En revanche, la représentation des processus dans les modèles climatiques régionaux contribue à l'incertitude des scénarios CH2018. En particulier, la prise en compte de l'effet du CO_2 sur la physiologie des plantes et la fermeture des stomates, étudié dans le cadre du projet, conduit à une réduction de l'évaporation en Europe centrale et septentrionale. Cette réduction entraine un effet rétroactif sur l'évolution future de la température et des températures extrêmes nettement plus élevées.

Selon les calculs, les besoins en irrigation de la Suisse vont doubler d'ici la fin du siècle sous l'effet du changement climatique. Ce signal provient principalement du Tessin, du Bas-Valais et de la région de Bâle. Toutefois, les rétroactions qui en résultent sur le cycle hydrologique et les indicateurs de sécheresse et de bilan hydrique étudiés sont faibles et principalement visibles dans le sud de l'Europe.
.

1   Introduction

Both soil moisture and evapotranspiration are key elements of the Earth system. In particular, evapotranspiration builds the link between the water, energy and carbon cycles and is thus highly relevant for climate and hydrological applications (e.g., Seneviratne et al. 2010). Soil moisture being the lower boundary for the atmosphere over land is impacting evapotranspiration through its influence on the partitioning of the available energy at the Earth surface into sensible and latent heat fluxes. Soil moisture also constitutes the water that is directly available to plants and thus the main water source of most ecosystems. Also, the amount of water stored in the soil impacts the generation of runoff and groundwater recharge.

The terrestrial water balance without considering lateral exchange can be expressed as:

$$\frac{dS}{dt} = P - E - R_s - R_g \qquad (1)$$

where dS/dt is the change of terrestrial water storage, P is precipitation, E is evapotranspiration, R_s is surface runoff, and R_g is groundwater flow. S contains moisture stored in the soil, surface water, snow, ice cover and water stored in biomass. Similarly, the water balance can also be expressed for a surface soil layer only, where, depending on the considered depth, R_g becomes drainage or baseflow. Evapotranspiration E correspondingly includes bare soil evaporation, transpiration from plants, evaporation from the interception storage, snow sublimation, and evaporation from surface water.

The energy balance over land (without considering lateral exchange, e.g., advection of energy) can be expressed as:

$$\frac{dH}{dt} = R_n - \lambda E - SH - G \qquad (2)$$

where dH/dt is the change of energy within the considered surface soil layer, R_n is net radiation, λE is latent heat flux, SH is sensible heat flux, and G is ground heat flux to deeper soil layers. From these two equations, it can be seen that the water and energy cycles are coupled through evapotranspiration (cf. the terms E and λE). Through its impact on the energy partitioning at the surface, soil moisture plays a key role both for the water and energy cycles. Moreover, it is linked to several biogeochemical cycles (e.g. carbon and nitrogen cycles) through the coupling between transpiration and photosynthesis of plants (e.g., Seneviratne et al. 2010; Wolf et al. 2013).
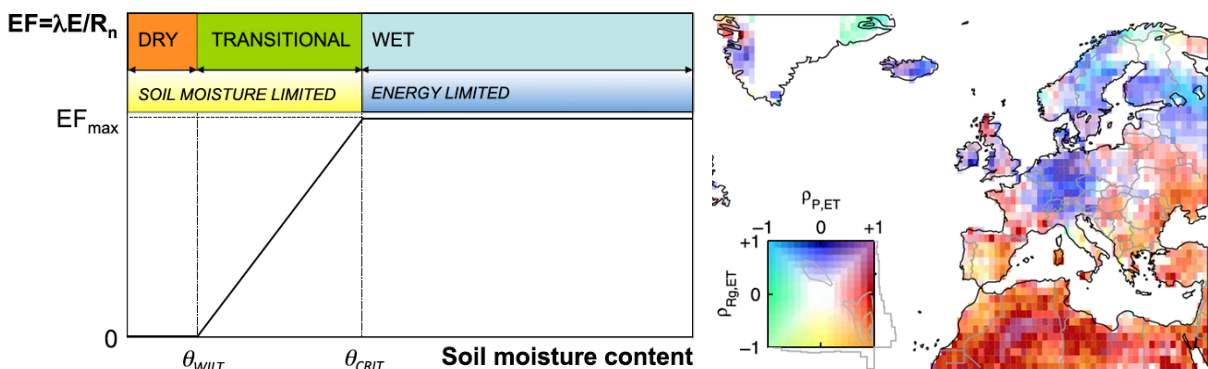
Figure 1: (left) Conceptual framework for the dependence of evaporative fraction on soil moisture within the different soil moisture and evapotranspiration regimes (from Seneviratne et al. 2010). (right) Controls on yearly evapotranspiration based on a land-surface model ensemble. Correlation between yearly evapotranspiration and global radiation ($\rho_{Rg,E}$), respectively precipitation ($\rho_{P,E}$), for the period 1986–1995. Each color corresponds to a unique combination of $\rho_{Rg,E}$ and $\rho_{P,E}$ (extract from Teuling et al. 2009). Note that E is denoted ET in this panel.

The impact of soil moisture on the climate system can be explained by its influence in soil moisture limited evapotranspiration regimes (Figure 1), which are linked to dry and

transitional soil moisture regimes (e.g., Koster et al. 2009; Seneviratne et al. 2010). With decreasing soil moisture, the remaining moisture becomes less accessible for plant uptake (and bare soil evaporation) and thus the fraction of available energy going into latent heat flux (and thus evapotranspiration) gets reduced, leading on the other hand to an increase in sensible heat flux (e.g., Seneviratne et al. 2010, 2006b) and consequently to feedbacks on temperature and precipitation (see Section 2.3).

2 Definitions and relevance

2.1 Soil moisture

Soil moisture is defined as the water stored in the unsaturated soil zone. It can either be expressed as volumetric soil moisture θ (i.e., the volume of water per soil volume, in m^3/m^3) or as water column height within a specific soil layer (in mm). The later definition is often used in land surface or hydrological models and is directly related to the water balance equation (Eq. 1)

2.1.1 Measurement methods and data basis

Soil moisture can be measured in-situ either using labor-intensive, non-continuous and/or destructive measurement techniques, as e.g., gravimetric sampling, or by use of electromagnetic sensors to establish continuous measurement time series. These ground measurements make use of different physical properties, such as permittivity and soil thermal properties, as well as change in mass and cosmic-ray neutrons to relate these characteristics to the soil water content. The in-situ techniques measure on the point scale and thus are (in absolute terms) representative for a limited soil volume only. They can have a high resolution in the vertical direction and, if continuously measured, a high temporal resolution (e.g., Mittelbach 2011). In Switzerland, in-situ measurement of soil moisture are available from the Swiss Soil Moisture Experiment network (SwissSMEX; Mittelbach 2011; Mittelbach and Seneviratne 2012), from the Soil Moisture in Mountainous Terrain research monitoring network (SOMOMOUNT; Pellet and Hauck 2017), and from WSL's Long-term Forest Ecosystem Research Programme (LWF). For an overview on available data for Switzerland, see Seiz and Foppa (2007) and updates thereof.

Moreover, soil moisture can be retrieved from active and passive microwave remote sensing. Similar to electromagnetic ground-based soil moisture sensors, microwave remote sensing methods use the large difference of the dielectric permittivity of water compared to solid material. Water affects the dielectric properties of the soil, which in turn affect emissivity and reflectivity of the uppermost soil layer (Schmugge et al., 2002). Recently, attempts have been made to merge various microwave sensors to develop a long-term climatological record of remote-sensing soil moisture (Liu et al., 2012). This has been achieved within the European Space Agency (ESA) Climate Change Initiative (CCI) soil moisture, and the current version of the product covers an almost 40-year time period, with a daily temporal and a 0.25° spatial resolution (Dorigo et al., 2017).

Finally, soil moisture estimates can also be derived by means of land-surface modelling. In this case, a physical model is forced with observed atmospheric variables and soil moisture (as well as other land-surface variables) are calculated (e.g., Balsamo et al. 2015; Orth and Seneviratne 2015).

2.1.2 Spatio-temporal characteristics

Soil moisture dynamics are characterized by a substantial amount of persistence (also called memory), which is mostly due to its integrative behavior (e.g., Seneviratne et al. 2006a; Orth and Seneviratne 2012; Seneviratne and Koster 2012). Persistence of soil moisture is relevant for the climate system due to the role of soil moisture in the partitioning between the latent and sensible heat fluxes and the consequent impacts on the near-surface atmospheric conditions, boundary layer stability and possibly precipitation (see Section 2.3). Moreover, soil moisture persistence may help in seasonal forecasting (e.g., Koster et al. 2010; van den

Hurk et al. 2010), as well as for the long-term predictability of soil moisture itself (Nicolai-Shaw et al., 2016).

The spatio-temporal variability of soil moisture is impacted by the heterogeneity of different characteristics, such as soil texture, vegetation, topography and meteorological conditions. For Switzerland, Mittelbach and Seneviratne (2012) provided an analysis of the time-invariant and the time-varying contributors to spatio-temporal variability based on the SwissSMEX stations. The spatial variance of absolute soil moisture over time is thereby decomposed into contributions from the spatial variance of the (time-invariant) mean soil moisture at all sites, and time-varying components that are related to soil moisture dynamics. The analysis revealed that the time invariant term contributes on average 94% of the spatial soil moisture variance at any point in time. On the other hand, the spatial variance of the temporal anomalies (with respect to the long-term mean) is relatively limited and constitutes on average 9% of the total variance. This comparable consistent regional signal in the soil moisture dynamics is to a large extent driven by meteorological and climatological factors, while the time invariant mean soil moisture levels are influenced by local factors (e.g., soil properties, local slope). These results were confirmed using data from five additional soil moisture networks, which also revealed that the temporal anomalies tend to have a minimum in the spatial variability for intermediate conditions (Brocca et al., 2014).

2.2 Evapotranspiration

Evapotranspiration is defined as the flux of water that is returned to the atmosphere from the Earth's land and ocean to the atmosphere. Over land, it comprises plant transpiration and evaporation. The relative importance of these two components has recently been under debate (Coenders-Gerrits et al., 2014; Jasechko et al., 2013). Based on a compilation of over 80 studies, Schlesinger and Jasechko (2014) conclude that transpiration accounts for 61% ($\pm$15%) of evapotranspiration. Further, evaporation can be split into bare soil evaporation, canopy interception loss and snow sublimation (e.g., Miralles et al. 2011). The relative importance of these components is again quite diverse between data sets (e.g., Schwingshackl et al. 2017).

2.2.1   Measurement methods and data basis

In-situ methods for measuring evapotranspiration include lysimeters (e.g., Rana and Katerji 2000; Seneviratne et al. 2012a) as well as eddy covariance (EC) flux measurements (e.g., Baldocchi et al. 2001). Despite being the best-established reference methods, the spatial and temporal extent of these observations is scarce. For Switzerland, lysimeter measurements are e.g., available from the Rietholzbach research catchment (Hirschi et al., 2017; Seneviratne et al., 2012b), as well as from lysimeter installations in Basel and Reckenholz. Moreover, Swiss FluxNet[1] combines various EC flux measurement sites in Switzerland. In particular, EC measurements are also available at the already mentioned Rietholzbach research catchment, where they have been evaluated with lysimeter measurements as well as catchment water balance estimates (Hirschi et al., 2017).

Beside these ground observations, diagnostic techniques (e.g., catchment water balance estimates), land-surface modeling and re-analyses, as well as remote sensing-based algorithms can provide estimates of evapotranspiration (Jiménez et al., 2011; Michel et al., 2016; Miralles et al., 2016; Mueller et al., 2013).

2.2.2   Drivers of evapotranspiration

The main external drivers for evapotranspiration are incident solar radiation and precipitation/moisture availability (e.g., Teuling et al. 2009; Seneviratne et al. 2010). Accordingly, one can distinguish between soil moisture-limited and energy-limited evapotranspiration regimes (Figure 1). In the energy-limited evapotranspiration regime, where soil moisture is abundant (wet soil moisture regime with $\theta > \theta_{CRIT}$), evaporative fraction

---

[1] www.swissfluxnet.ch/

(i.e., the fraction of available energy going into latent heat flux, $EF = \lambda E/R_n$) is independent of the soil moisture content and evapotranspiration variations are driven by available energy. In the soil moisture-limited evapotranspiration regime (transitional and dry soil moisture regimes, $\theta < \theta_{CRIT}$), soil moisture content provides a first-order constraint on evapotranspiration until it reaches the wilting point (θ_{WILT}). Below this point, no evapotranspiration takes place anymore. In the transitional climate regime, soil moisture strongly constrains evapotranspiration variability and thus influences resulting feedbacks to the atmosphere (Seneviratne et al., 2010).

Regional (and temporal) variations in the main drivers of evapotranspiration (i.e., radiation and moisture) need to be considered to understand trends and variations in evapotranspiration. For Central Europe, correlations between evapotranspiration and radiation are strong (Figure 1), and trends derived from weighing lysimeters and river-basin water budgets follow trends in radiation, indicating a currently energy-controlled evapotranspiration regime (Seneviratne et al., 2010; Teuling et al., 2009). Drivers of evapotranspiration are however dynamic and can change over the course of a year up to decadal time scales, for instance due to projected shifts in climate regimes (Seneviratne et al., 2006a). Further controls for evapotranspiration include advection, turbulent transport, leaf area, plant-available water, nutrient availability, CO_2 concentration, atmospheric humidity, wind speed and water use changes (e.g., Zhang et al. 2001; Teuling et al. 2009).

Vegetation imposes an additional control on evapotranspiration by regulating soil-to-atmosphere water exchanges. There is ample empirical evidence that evapotranspiration rates, or evaporative fraction, are strongly influenced by the type of vegetation cover (Bonan, 2008; Chen et al., 2018; Teuling et al., 2010; Williams et al., 2012). Evapotranspiration is on average higher in forest compared to unmanaged grassland or rainfed crops (Ambrose and Sterling, 2014; Chen et al., 2018; Meier et al., 2018; Vanden Broucke et al., 2015). Converting forest to grass tends to decrease evapotranspiration and enhance sensible heating, therefore warming the near-surface atmosphere (Bonan, 2008; Davin et al., 2007). During heat waves, however, the temporal response of forests and grassland is contrasted (Teuling et al., 2010). Initially, heating is twice as high over forest than over grassland due to increased evapotranspiration over the latter. Later, this enhanced evapotranspiration of grassland accelerates soil moisture depletion and induces a critical shift in the regional climate system that leads to increased heating over grassland while the conservative water use of forest mitigates the heat of the longer-lasting events. Over the Swiss Plateau, historical land-use change has been investigated by Schneider et al. (2004). Using model simulations, they report that land-use change has increased albedo, leading to a decrease of net radiation. Also, the partitioning of incoming energy was altered, favoring latent heat rather than sensible heat for present-day land use.

In addition to land cover change, forest and crop management may also impact evapotranspiration (e.g., Davin et al. 2014; Naudts et al. 2016; Seneviratne et al. 2018). In Switzerland, as in the rest of Europe, forestry activities have favored coniferous trees at the expense of native broadleaf species (McGrath et al., 2015). Conifers evaporate less than deciduous broadleaf trees according to limited but consistent evidence (Ambrose and Sterling, 2014; Duveiller et al., 2018; Renaud et al., 2011). Converting deciduous forests to coniferous forest thus results in a decrease of evapotranspiration, which together with associated changes in albedo and canopy roughness may have contributed to a warming of the atmosphere (Naudts et al., 2016). Concerning cropland management, irrigation plays a particularly important role by enhancing evapotranspiration compared to rainfed crops (Ambrose and Sterling, 2014). Irrigation will likely become more necessary due to climate change also in Switzerland, with consequent impact on evapotranspiration. Currently, the need for irrigation is in particular distinct in western Switzerland, the lower Valais and some inner-alpine valleys. Overall, about 41% of the arable land and 26% of the agricultural land exhibits a need for irrigation (Fuhrer and Jasper, 2009). One positive side effect of irrigation lies in the mitigation of extreme temperatures. The impact of irrigation appears particularly strong for the hot tail of the temperature distribution (Thiery et al., 2017). The cooling is

predominantly caused by an increase in evaporative fraction, with only a minor influence of reduced net radiation to the surface. Other management practices, such as no-till farming can also play an important role. In no-till systems, a crop residue cover is retained which tends to reduce evaporation from the soil, while also increasing albedo. During hot days however, the albedo effect is the dominating factor, which can lead to a local cooling of the order of 2°C (Davin et al., 2014).
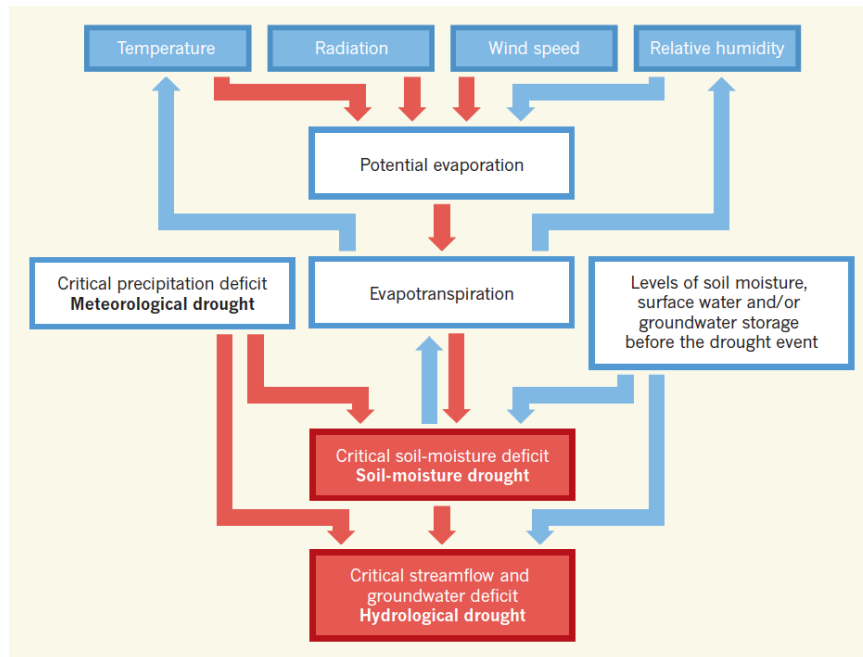
2.3 Drought

2.3.1   Drought indices and drivers

Due to the widespread lack of in-situ soil moisture observations, various soil moisture proxies and specifically drought indices have been developed in the past (e.g., Heim 2002; Dai 2011; Seneviratne et al. 2012; see also
Table 1). These consider different aspects of drought. Commonly, one distinguishes between meteorological drought, which refers to a deficit of precipitation, soil moisture drought (often called agricultural drought), which refers to a deficit of (mostly root zone) soil moisture, and hydrological drought, which refers to negative anomalies in streamflow, lake, and/or groundwater levels (Heim, 2002). Note that these indices are not restricted to quantify dryness, but can also be used to characterize wet conditions.

The primary cause for drought is often lack of precipitation, which led to the definition of meteorological drought indices covering the aspect of a water deficit on the supply side (Figure 2). On the demand side, increased evapotranspiration due to enhanced radiation, wind speed, or vapor pressure deficit (itself linked to temperature and relative humidity) can further intensify the water shortage and lead to critical soil moisture values and thus agricultural drought. For Europe, a statistically significant and consistent positive contribution of evapotranspiration to storage anomalies during summer drought was found based on observational catchment data (Teuling et al., 2013). Similarly, Stegehuis et al. (2013) found that warm summers are preceded by an increase in latent heat flux in early spring. Moreover, the increase in available energy during warm summers results in an excess of both latent and sensible heat fluxes over most of Europe. As an example, the summer of 2003 showed for the Rietholzbach catchment in northeastern Switzerland an evapotranspiration excess in June that contributed 60% of the water storage deficit of that month and thus represented the main driver initiating the following summer drought (Seneviratne et al., 2012b). With drier climate conditions and under strong droughts, the amplifying role of evapotranspiration will however reduce and soil moisture can also become limiting for evapotranspiration, thus restricting further soil moisture depletion and consequent reduction of evaporative cooling (e.g, Miralles et al. 2014). Furthermore, pre-conditioning (pre-event soil moisture, surface and/or groundwater storage) can contribute to the emergence of agricultural and hydrological droughts. This is related to the inherent characteristic memory of these water stores (e.g., Koster and Suarez 2001; Seneviratne et al. 2006a; Orth and Seneviratne 2012) and their specific response times to drought forcing (e.g., Fleig et al. 2011). Apart from these more local drought drivers, summer drought in Europe are often accompanied by winter/spring rainfall deficits over Southern Europe, which spreads northward through atmospheric transport of anomalously warm and dry air during southerly wind episodes (Vautard et al., 2007; Zampieri et al., 2009).

Figure 2: Drivers of soil-moisture and hydrological drought, with red arrows showing factors that contribute to drought, and blue arrows factors that counteract it (from Seneviratne 2012). Also visible is the central position of evapotranspiration in governing and responding to drought conditions.

As can be seen from Figure 2, critical soil moisture deficits can further propagate into critical streamflow and groundwater deficits. The depletion of soil moisture storage during drought episodes causes a decreased recharge to the groundwater system, resulting in declining groundwater levels (e.g., Van Loon 2015). This reaction of groundwater is often delayed and smoothed, but critical levels often show long periods of below-normal. In turn, both the low soil moisture content as well as low groundwater levels also lead to decreased streamflow. The severity of hydrological drought is highly dependent on processes related to storage changes in soil and groundwater, snow and glaciers (e.g., Staudinger et al. 2014; Van Loon et al. 2015) as well as catchment properties (Van Lanen et al., 2013), and may thus be spatially diverse even within the area of Switzerland (BUWAL et al., 2004).

For the recent national climate change scenarios, several meteorological and agricultural drought indices have been considered (CH2018 technical report, Chapter 6.7 therein), which are extended by additional indices within Hydro-CH2018 (Table 1, see also Section 5).

CDD shows the maximum number of consecutive days without rain (i.e., below a given threshold of 1 mm/d) within a considered period. Here, *CDD* is calculated on a seasonal timescale (i.e., for DJF, MAM, JJA, or SON as a whole). Another commonly used meteorological drought index is the standardized precipitation index (SPI) which is derived by fitting and transforming a long-term precipitation record into a normal distribution with zero mean and unit standard deviation (Lloyd-Hughes and Saunders, 2002). SPI values of -0.5 to -1 correspond to mild droughts, -1 to -1.5 to moderate droughts, -1.5 to -2 to severe droughts, and below -2 to extreme droughts. Similarly, values from 0 to 2 correspond to mildly wet to severely wet conditions, and values above 2 to extremely wet conditions. SPI can be computed over several timescales (e.g., 3, 6, 12, or more months) and thus indirectly considers effects of accumulating precipitation deficits (or excess). Here, the 3-month timescale is used (3-month SPI, denoted *SPI3*).

Table 1: Drought and water-balance indices used within CH2018 or Hydro-CH2018 "Water balance and droughts".

Index	Description	CH2018	Hydro-CH2018	References

CDD	Maximum number of consecutive dry days ($P<1$ mm/day)	X	X	Frich et al. (2002); Alexander et al. (2006); Tebaldi et al. (2006)
SPI3	Standardized precipitation index for 3-months accumulated precipitation	X	X	McKee et al. (1993); Lloyd-Hughes and Saunders (2002)
P-E	Precipitation minus evapotranspiration	X	X	Byrne and O'Gorman (2015); Greve and Seneviratne (2015)
SMA	Standardized soil moisture anomalies	X	X	Orlowsky and Seneviratne (2013)
SRA	Standardized runoff anomalies		X	Gudmundsson and Seneviratne (2015, 2016b)
E	Simulated evapotranspiration		X	

Precipitation minus evapotranspiration (*P-E*) describes the net flux of water between atmosphere and land by including the influence of both atmospheric supply and demand. Here, seasonal averages of *P-E* are considered to represent water availability. Actual evapotranspiration, which results from atmospheric forcing and simulated soil moisture limitation on evapotranspiration, is used; compared to potential evapotranspiration, it is less prone to overprediction (Milly and Dunne, 2016). The index is categorized as an agricultural drought index, although it neglects storage changes and runoff. Moreover, we also evaluate simulated evapotranspiration *E* alone. Standardized soil moisture anomalies (*SMA*) are also a measure for the evaluation of agricultural drought based on simulated total column soil moisture. Monthly *SMA* values are calculated with respect to the monthly means of the reference period (1981–2010) and standardized by the monthly standard deviations of the reference period (Orlowsky and Seneviratne, 2013); these values are then seasonally averaged. *SMA* integrates the effects of precipitation forcing, evaporative demand, and soil moisture persistence.

For hydrological drought, standardized runoff anomalies (*SRA*) are considered. *SRA* is calculated by log-transforming the monthly runoff time series (Gudmundsson and Seneviratne, 2015b, 2016b). Subsequently, the monthly long-term mean of the reference period is subtracted from the log-transformed time series, and divided by the monthly standard deviation of the reference period.

2.3.2 Impacts

Droughts can have multiple impacts on environment, society, and the economy. Based on the European Drought Impact report Inventory (EDII[2]), Stahl et al. (2016) revealed that drought impacts on agriculture and public water supply dominate in the drought impact reports for most countries and for all major drought events since the 1970s, while the number and relative fractions of reported impacts in other sectors can vary regionally and from event to event. The inventory shows severe impacts in southern Europe (particularly on agriculture and public water supply) and sector-specific impacts in central and northern Europe (e.g., on forestry or energy production) that can to a large extend be linked to meteorological drought indicators (Blauhut et al., 2015). Furthermore, drought can act as triggers for other natural hazards at the sub-continental scale, including above normal wildfire activity (Gudmundsson et al., 2014).

Drought impacts on agriculture are also expected for Switzerland, in particular also with respect to projected decreases in the frequency of wet days, and shorter return times of heat waves and droughts (e.g., Calanca and Fuhrer 2005; Fuhrer et al. 2006). Crops currently cultivated in Switzerland have been selected for cultivation in temperate, humid conditions. Their sensitivity to precipitation deficits during the main growing season is high, as demonstrated by the yield losses in the most affected areas in 2003 and 2015 (BAFU, 2016; Fuhrer et al., 2006; Keller and Fuhrer, 2004; ProClim, 2005). Using a stochastic soil moisture

---

[2] www.geo.uio.no/edc/droughtdb/index.php

model, Calanca (2004) showed that in the past, about 20% of the years exhibited soil moisture conditions during the growing season in northern Switzerland that were close to the permanent wilting point, suggesting potential crop losses due to drought. The economic and financial losses in the agricultural sector due to drought years can be substantial. The widespread and long-term (July to October) drought in 1947 caused drops in wheat yields in northwestern and central Europe by 25–35% relative to the long-term average, and fodder became scarce and expensive throughout the continent (Schorer, 1992). More recently, the 2003 summer drought lowered yields of various crops and fodder cereals by about 20% relative to the mean for 1991–1999, with most pronounced losses in the western and northern Switzerland (Keller and Fuhrer, 2004; ProClim, 2005). Recent results show that the combined non-linear effect of moisture availability and temperature appears most relevant for explaining crop yield variability (Zscheischler et al., 2017).

Impacts of drought episodes may also depend on the (cultivated) plant species (BAFU, 2016). In grasslands, droughts (and associated increase in sunshine, temperature, and vapor pressure deficit) may lead to carbon loss, while increased carbon uptake may be found especially in deciduous forests (De Boeck and Verbeeck, 2011). This difference could be attributed to better access of forest ecosystems to water reserves of deeper soils. Thus, the warmer and sunnier conditions naturally associated with droughts can either improve growth or aggravate drought-related stress, depending on water reserves (De Boeck and Verbeeck, 2011). Similarly, it has been shown that anomalies in vegetation indices (NDVI, FPAR, LAI) during drought episodes are generally larger over grassland than over forests (Nicolai-Shaw et al., 2017).

Through feedback with the atmosphere, the prevailing dry conditions may further enhance air temperatures and trigger heat extremes (e.g., Seneviratne et al. 2006; Hirschi et al. 2011; Mueller and Seneviratne 2012; Quesada et al. 2012; Miralles et al. 2014; Whan et al. 2015). In dry and transitional soil moisture regimes (see Figure 1), the decrease of soil moisture during drought episodes leads to a redistribution of the surface energy with more energy going into sensible heating and less into latent heat flux (i.e., evapotranspiration). This soil moisture-temperature feedback, together with persistent atmospheric pressure patterns, large-scale horizontal heat advection and enhanced entrainment of warm air into the boundary layer may result in a progressive accumulation of heat as occurred during the 2003 and 2010 heat waves (Miralles et al., 2014b). The impact of such heat waves on human health is substantial, with death tolls of 40'000 and 55'000 for these two events (e.g., García-Herrera et al. 2010; Barriopedro et al. 2011). For the future, soil moisture-temperature effects may become even more dominant, particularly in regions that will undergo a drying trend. The contribution of the soil moisture-temperature effect is in particular strong in Central Europe, where it contributes more than 70% to the amplified warming of the hottest days compared to projected global mean temperature (Vogel et al., 2017), as well as in the Mediterranean, where 25% of the climate change signal for extreme temperature is due to the soil moisture effect (Seneviratne et al., 2013).

Further impacts of droughts and associated heat waves may include animal health, air quality, water resources and energy production (BAFU, 2016; BUWAL et al., 2004; ProClim, 2005), as well as building stability (Corti et al., 2009). Also due to these multi-faceted impacts of droughts on various sectors, the topic received increasing attention during the past years, e.g. within the NRP 61 DROUGHT-CH project[3] for Switzerland and within the EU-FP7 DROUGHT-RSPI project[4] on the European scale (Tallaksen et al., 2015).

---

[3] www.nfp61.ch/de/projekte/projekt-drought-ch
[4] www.eu-drought.org

3 Historical changes and past events in Central Europe and Switzerland
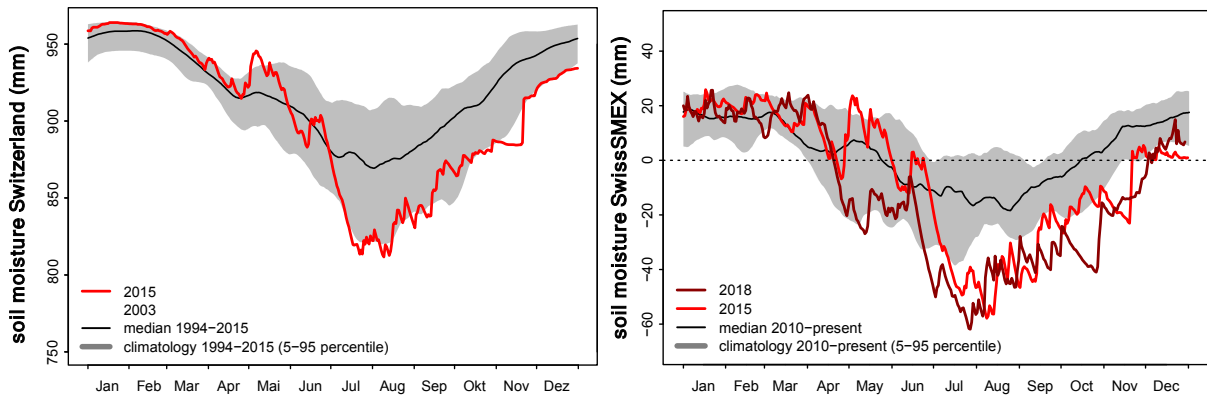
3.1 Soil moisture and drought

Results from various studies present contrasting conclusions regarding past drought trends in Europe, depending on the applied drought index and the considered time period (e.g., Lloyd-Hughes and Saunders 2002; Dai et al. 2004; van der Schrier et al. 2006; Gudmundsson and Seneviratne 2015a, 2016a). For Central Europe in particular, observed historical trends in dryness are inconclusive and associated with large uncertainties (e.g., Seneviratne et al. 2012b; Orlowsky and Seneviratne 2013; Gudmundsson and Seneviratne 2015a, 2016a; Gudmundsson et al. 2017). Trends vary spatially, with some increases in dryness (*SMA*, *CDD*, Palmer Drought Severity Index) in part of the region but also regional variation in dryness trends and dependence of trends on the considered index or time period (Seneviratne et al., 2012a). Also, Switzerland does not show significant historical trends in dryness, though a tendency towards drying (based on P-E; CH2018). Generally, Central Europe (and Switzerland) is located between a drying region in the south and a wetting region in the north, which can be clearly seen in observations of precipitation, *SPI* and streamflow. This change pattern has been attributed to climate change (Gudmundsson et al., 2017; Gudmundsson and Seneviratne, 2015a) and is also present in future simulations (see below).

Despite this lack of confidence on drought trends, several major drought events have been reported for Central Europe and Switzerland (Pfister, 1999; Pfister and Rutishauser, 2000; Schorer, 1992). The most severe drought experienced on the Swiss Plateau in the last 100 years was 1947, which was peculiar in terms of spatial extent, the spatial coherency of the anomalous dry phases as well as the persistence of the negative precipitation anomaly (Calanca, 2007). In order of severity, this event was followed by the droughts of 1906, 1949, 1911, 1962, 2003 and 1976. Note that 2003 is only ranging sixth in terms of dryness in this ranking, although the summer temperature anomaly was by far still record breaking[5] (Bader, 2004; ProClim, 2005). More recently, 2015 showed anomalously dry and hot conditions (BAFU, 2016; MeteoSchweiz, 2016; Orth et al., 2016).

Figure 3 (left panel) displays the temporal evolution of soil moisture in Switzerland (based on the observation-driven Simple Water Balance Model, SWBM; Orth and Seneviratne 2015) for the drought years 2003 and 2015, as well as the climatology of 1994–2015. Both years start with comparable wet soils and then show a rapid decline in soil moisture from June onwards. The soil moisture values during both summers range around or below the 5% percentile of the climatology. 2015 experienced a longer dry anomaly, which lasted until autumn/winter. 2003 showed more variation and recovery phases, but an overall stronger anomaly (see also BAFU 2016). Note that in contrast for a larger Central European domain, analyses of precipitation and SWBM-derived soil moisture revealed that the 2015 event was drier than 2003 (Orth et al., 2016).

---

[5] www.meteoschweiz.admin.ch/home/klima/klimawandel-schweiz/temperatur-und-niederschlagsentwicklung.html

Figure 3: (left) Evolution of soil moisture in the SWBM (area average over Switzerland) in the drought years 2003 and 2015, and in relation to the long-term climatology. (right) Evolution of the averaged soil moisture anomalies (integrated over the top 50 cm of the soil) in the drought years 2015 and 2018 at the SwissSMEX grassland stations, and in relation to the long-term climatology (without the dry years 2015 and 2018).

In 2018, Switzerland and large parts of Central and Northern Europe were again affected by exceptional and extended summer dryness (MeteoSchweiz, 2018). Apart from a large precipitation deficit, enhanced evapotranspiration led to substantial negative values of the water balance. This combined effect is clearly visible in the soil moisture measurements from the SwissSMEX network (available since 2009, see Figure 3 right panel). Compared to 2015, the summer 2018 event in Switzerland was characterized by an earlier onset of the dry conditions in spring and partly falls below the 2015 anomaly at the height of the drought (based on averaged soil moisture anomalies at the SwissSMEX grassland sites).

3.2 Evapotranspiration

Historical trends in evapotranspiration are difficult to assess as long-term measurements from lysimeters or EC towers are scarce. In regions where evapotranspiration correlates with radiation (see Section 2.2.2), trends in radiation (due to tropospheric air pollution-induced ''dimming'' and ''brightening''; Wild et al. 2005, 2009) are expected to impact evapotranspiration. This is the case in Central Europe (Figure 1), where trends derived from weighing lysimeters and river-basin water budgets follow trends in radiation, showing all a consistent convex temporal behavior with a decline up to the 1980s (though delayed in the lysimeter data) followed by an increase (Teuling et al., 2009). Also Stegehuis et al. (2013) report a positive trend for latent heat flux over Europe after 1982, consistent with increased solar radiation due to a decrease in cloudiness and a reduction in atmospheric aerosols concentration (Wild et al., 2009). On the larger scale, also northern latitudes (30°N–90°N) show a monotonic and statistically significant rise in evapotranspiration since the 1980s (Miralles et al., 2014a). Note that on the global scale, internal multi-year climate variability due to ENSO provide additional forcing for observed trend oscillations in evapotranspiration (Jung et al., 2010; Miralles et al., 2014a; Mueller et al., 2013).

4   Projected changes in Central Europe and Switzerland

4.1 Soil moisture and drought

Recent studies suggest that future drought projections should rely on direct climate model output of the water cycle (e.g., simulated soil moisture as used for *SMA* or actual evapotranspiration as used for *P-E* and *E*, see below), as a posteriori off-line metrics tend to overestimate drying trends (e.g., Berg et al. 2017; Milly and Dunne 2017). Climate model projections show an increase in dryness (based on *CDD*, *SMA*) and in short-term droughts in Central Europe by the end of the century under pessimistic emission scenarios (Orlowsky and Seneviratne, 2013; Seneviratne et al., 2012a; Sheffield and Wood, 2008; Tebaldi et al., 2006). These projections based on the full Coupled Model Intercomparison Project Phase 5 (CMIP5) model ensemble might possibly underestimate the future dryness trend in Central Europe, as models best representing past drought events showed stronger future drying than

the full model ensemble in that region (Orth et al., 2016). On the other hand, a recent study by Vogel et al. (2018) suggests that in a constrained CMIP5 model ensemble, summer precipitation in Central Europe is more likely to stay close to present-day levels as compared to the full model ensemble.

For the Alpine region and Switzerland, studies also report an increase in drought frequency (e.g., Calanca 2007) and a tendency toward increasing drought risk and longer dry spells in summer (CH2011). Recently, the new CH2018 climate change scenarios refined these regional projections based on regional climate model (RCM) projections from the European branch of the Coordinated Regional Climate Downscaling Experiment (EURO-CORDEX). Based on four drought indices, these projections show a tendency towards an increase in dry spell lengths (*CDD*) and tendencies towards drying in summer (*SPI3*, *P-E*, *SMA*), as well as wetting in winter (but only when storage effects are neglected, i.e., for *SPI3* and *P-E*) for Switzerland. These responses are strongest for the RCP8.5 emission scenario and for the latest scenario period around 2085. As for the observed trends, Switzerland is at the edge of an enhancing north-south contrast on the European scale, with a severe drying in southern Europe (in summer/autumn) and wetting in northern Europe (in winter/spring, CH2018). These scenarios will be further evaluated in Section 5 using observational data as well as additional drought and water balance indices (cf. Table 1)

4.2 Evapotranspiration

Future projections for evapotranspiration have been less widely reported than for soil moisture or traditional drought indices, despite the importance of the variable as a driver of drought and for land-climate interactions. It has been shown that the future response of summer evapotranspiration over Europe is strongly dependent on how climate models represent the role of soil moisture and radiative energy at the land surface on evapotranspiration in the present climate (Boé and Terray, 2008). Models with a strong limiting effect of soil moisture on evapotranspiration in the present climate generally respond with a future decrease of evapotranspiration whereas the other models show an increase. More recent results based on CMIP5 show a consistent picture with models showing both increase and decrease in latent heat flux in Central Europe (Vogel et al., 2018). Apart from these uncertainties in projections of evapotranspiration, the simulation of this variable is also associated with systematic biases. CMIP5 models tend to overestimate evapotranspiration in most regions, especially also in Europe (Mueller and Seneviratne, 2014). This appears connected with an overestimation of precipitation as compared to reference data sets and may explain observed temperature biases as well. An observationally constrained ensemble indicates a reduced risk for severe drying in Central Europe with respect to *P-E* (Padrón et al., 2019).

When considering evapotranspiration as a measure for projected changes in the water cycle, it is important to rely on direct climate model output instead of a posteriori offline metrics or offline simulations which use estimates of potential evapotranspiration as input. Due to biases in the estimation of the change of potential evapotranspiration with climate change, excessive increases in actual evapotranspiration are produced, because the system is not constrained by actual water availability (Milly and Dunne, 2017), and because the effect of stomatal conductance reductions commonly induced by increasing atmospheric CO_2 concentrations is neglected (Milly and Dunne, 2016). A similar effect appears when considering changes in the aridity index (i.e., the ratio of potential evaporation to precipitation) to increased CO_2 concentrations (Greve et al., 2017). Overall, this results in offline metrics being systematically and substantially overestimating future drying trends.

On smaller spatial scales, patterns of evapotranspiration changes appear dependent on the spatial distribution of soil moisture as affected by slope, land-use and soil type (Calanca et al., 2006; Jasper et al., 2006).

5   Evaluation of the CH2018 scenarios

5.1 CH2018 baseline results and motivation

"In summer, a reduction in wet days and a tendency toward longer dry spells (meteorological droughts, i.e., periods with no rain) is expected in response to strong warming (RCP8.5 at the end of the 21st century, low to medium confidence). In addition, there will be an increasing evaporative demand, which is projected to lead to more pronounced agricultural droughts (drier soils, medium confidence). In comparison to temperature and precipitation extremes, the extent of the drying remains more uncertain." (CH2018)

This statement from the Executive Summary of the CH2018 technical report highlights the inherent uncertainties of current drought projections for Switzerland. The extent of the projected summer drying remains uncertain (both insignificant and very strong changes cannot be excluded) and partly depends on the region. This is on one hand related to the fact that Switzerland is located between southern Europe that is projected to experience a severe increase in drought risk, and northern Europe that will receive more winter precipitation. On the other hand, large natural climate variability and model uncertainties in the representation of key processes (e.g., strength of soil moisture-atmosphere feedbacks, circulation changes), as well as factors such as aerosol forcing, plant-physiology, irrigation, and land-use changes contribute to the uncertainty in these projections.

Here, we will re-evaluate these CH2018 scenarios and their uncertainties using observation-based drought and water-balance indices (Section 5.3), the relation of these indices to global warming and policy-relevant temperature targets (Section 5.4), as well as mechanistic model experiments to highlight their sensitivity to different processes not considered in the CH2018 scenarios (Section 5.5 – 5.7).

5.2 Methods

5.2.1   Model data

The CH2018 multi-model ensemble is based on the EURO-CORDEX RCM simulations (Jacob et al., 2014). The simulations cover the European domain and the 1971–2099 time period. Here, we focus on the historical simulations up to 2005, followed by the RCP8.5 scenario. Lateral boundary conditions and sea surface temperatures (SSTs) are provided by a set of global climate models (GCMs) from the CMIP5 ensemble. Within CH2018, the GCM–RCM model chains were quality controlled and models with obvious issues were excluded from the ensemble (details can be found in the CH2018 technical report, cf. Table 4.1 therein). Only the simulation with the higher resolution is used for RCMs for which both the 0.11° and 0.44° resolutions are available. This resulted in 21 GCM–RCM model chains that are considered in the CH2018 multi-model ensemble.

In addition to the CH2018 multi-model ensemble, dedicated experiments with the regional climate model COSMO-CLM[2] (Davin et al., 2011, 2016; Davin and Seneviratne, 2012) are performed in order to explore the role of processes that are not included in the CH2018 models. Namely, none of the CH2018 models include a representation of irrigation and of the CO_2 effect on plant stomatal conductance (referred as to the plant physiological effect in the following). To test the impact of these processes the following experiments were performed:
   (1) a reference simulation with the same setup as for the EURO-CORDEX model ensemble used in CH2018;
   (2) one simulation accounting for the plant-physiological effect;
   (3) one simulation applying irrigation over crop areas (using the present-day distribution of crops equipped for irrigation).

COSMO-CLM[2] couples the Consortium for Small-scale Modeling (COSMO) atmospheric model in Climate Mode (so called COSMO-CLM) to the Community Land Model (CLM). Here we use the version 5.0 of COSMO and the version 4.0 of CLM (Oleson et al., 2010) coupled

with OASIS3-MCT. The reference experiment is performed using the EURO-CORDEX setup as described above over the time period 1949–2099 with a resolution of 0.44°. The global climate model MPI-ESM-LR under RCP8.5 is used as driving GCM.

In CLM4.0, stomatal conductance is based on the Ball-Berry model (Oleson et al., 2010), which allows stomatal conductance to adjust to CO_2 concentrations. In the second experiment, the CO_2 concentration in the Ball-Berry equation is kept constant (at a level of 367 ppm), whereas in COSMO_PHYS the CO_2 concentration used in the Ball-Berry equation increases according to the RCP8.5 scenario.

In the third experiment, irrigation is simulated using a prognostic model in which irrigation amount is calculated for the irrigated part of the total crop area (total crop area remains identical to the reference simulation and is partitioned into a rainfed and irrigated fraction, the irrigation module being applied only to the latter). The amount of water added is calculated such that plant soil moisture stress is eliminated. For this experiment, the three time slices 1981–2010, 2020–2049 and 2070–2099 are available.

5.2.2 Observation-based indices

For the evaluation of the RCM simulations, various observational datasets are considered (

Table 2).

The use of multiple datasets (if available) for a given index provides a robust evaluation of the climate models, and allows to gain insight into the reliability of the observations and to set model biases in relation to the observational uncertainty.

5.2.3 Indices calculation, domain averaging and statistical evaluation

The drought and water balance indices (Section 2.3.1,
Table 1) used for the evaluation of the CH2018 multi-model ensemble and the COSMO-CLM^2 simulations are calculated at the grid-cell level of the individual models and of the observational datasets based on the definitions presented in Section 2.3.1. Except for *CDD*, the indices are thereby calculated on monthly time scale and then seasonally averaged. *CDD* is directly derived for the four seasons as a whole.

These seasonal grid-cell based indices are then area averaged using the five CH2018 Swiss domains (CH2018 technical report, Figure 2.6 therein) and three European regions defined in the Special Report on Extremes (SREX, Seneviratne et al. 2012b). In addition, the scaling of the indices with global mean temperature (Section 5.4) also considers the European regions from the PRUDENCE project (Christensen and Christensen, 2007).

Historical trends in the seasonal domain-averaged indices (see Section 5.3) are estimated by a simple linear regression based on the available time periods of the datasets, and significance of the slope estimate is evaluated using a two-sided Wald Test with t-distribution of the test statistic. A significance level of 5% is chosen. For the observation-based estimates, we in addition require a minimum temporal coverage of 15 years to evaluate trend significance. To test for differences in the means of individual model experiments (see Section 5.5), a Mann-Whitney-U test is applied (5% significance level).

Table 2: Overview on the observation-based datasets and what drought and water-balance indices evaluation they are applied (denoted with X).

Dataset	Description	Indices[6]					
		SPI	*CDD*	*P-E*	*SMA*	*SRA*	*E*
E-OBS	Gridded observations from E-OBS (Haylock et al., 2008)	X	X				
APGD	Alpine Precipitation Grid Dataset (Isotta et al., 2014)	X	X				
MeteoSwiss	Gridded high-resolution data (RhiresD, RhiresM[7]) from MeteoSwiss	X	X				
CCI-SM	Remote sensing data from the ESA CCI soil moisture project[8] (Dorigo et al., 2017)				X		
LandFlux-EVAL	LandFlux-EVAL Evapotranspiration benchmarking product (Mueller et al., 2013)			X[9]			X
GLEAM	Global Land Evaporation Amsterdam Model (GLEAM) estimation of the different components of land evapotranspiration from satellite data (Martens et al., 2017)						X
WECANN	Estimates of surface turbulent fluxes developed using a machine learning approach informed by remotely sensed solar-induced fluorescence (SIF) and other radiative and meteorological variables (Alemohammad et al., 2017)						X
Fluxnet-MTE	Upscaled observations from the global network of eddy covariance towers (FLUXNET) using a model tree ensemble (MTE) approach (Jung et al., 2009)						X
SWBM	Model-based estimates from the Simple Water Balance Model (SWBM, Orth and Seneviratne 2015) driven with observed meteorological forcing			X[9]	X	X	X
E-RUN	Observation-based gridded runoff estimates for Europe (Gudmundsson and Seneviratne, 2016b)					X	

5.3 Observational evaluation of CH2018 scenarios

In the following, we compare the agreement of the CH2018 multi-model ensemble and the COSMO-CLM[2] reference simulation (experiment (1) listed above) with observational datasets for the drought and water-balance indices listed in
Table 1. The comparisons are performed for the 1980–2017 time period (or shorter, depending on the availability of observational data) and are shown in Figure 4 – Figure 10. Corresponding results for the five CH2018 Swiss domains are shown in the Appendix (Figure

---

[6] See
Table 1
[7] See www.meteoswiss.admin.ch/content/dam/meteoswiss/de/service-und-publikationen/produkt/raeumliche-daten-niederschlag/doc/ProdDoc_RhiresD.pdf and www.meteoschweiz.admin.ch/content/dam/meteoswiss/de/Ungebundene-Seiten/Produkte/doc/ProdDoc_RhiresM.pdf
[8] www.esa-soilmoisture-cci.org/
[9] Combined with E-OBS precipitation

A1 – Figure A7), and mean bias plots for the same indices are presented in Figure A8 – Figure A21.

The maximum number of consecutive dry days (*CDD*) of the CH2018 multi-model ensemble agrees very well with the observations (Figure 4). In Switzerland, Northern and Central Europe, *CDD* lies around 10 days during summer, while it reaches about 50-60 days in Southern Europe. Both the observations and the CH2018 multi-model ensemble do not show significant trends in *CDD* (Figure 4, lower panel). COSMO-CLM^2 tends to overestimates *CDD* compared to the observations in Southern Europe, but is within the range of the CH2018 CORDEX models (Figure A8). Moreover, and in contrast to observations, COSMO-CLM^2 already exhibits a significant increase of *CDD* in Central and Southern Europe throughout the investigated time period (which is also projected for the future, see Section 5.5).
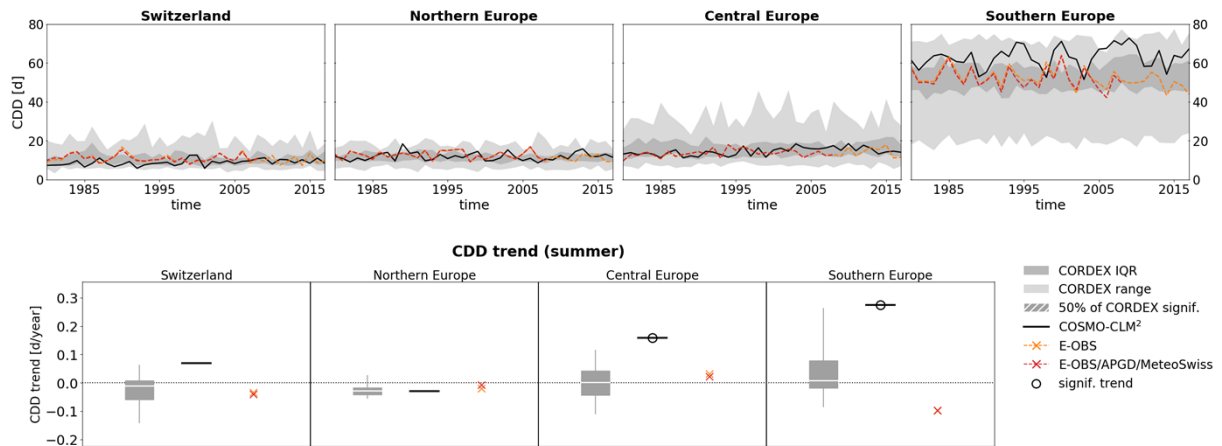

Figure 4: Historical evolution (upper panel) and historical linear trends (lower panel, see Section 5.2.3) of the maximum number of consecutive dry days (*CDD*) during summer (June, July, August) in Switzerland, Northern Europe, Central Europe, and Southern Europe during 1980–2017. The grey ranges in the upper panel indicate the evolution and spread of the CH2018 CORDEX models, the black line indicates COSMO-CLM^2, and the coloured dashed lines indicate the observations. The boxplots in the lower panel indicate the distribution of the CH2018 CORDEX models (white lines indicate the median, boxes the interquartile range and whiskers the 5th and 95th percentiles). Hatching for the CORDEX models indicates 50% of models having a significant trend consistent with the trend in the ensemble median, and circles indicate significant trends for COSMO-CLM^2 and the observations (based on a two-sided Wald test with t-distribution of the test statistic, significance level of 5%). For observational datasets it is additionally required that they span a time period of at least 15 years.

The evolution of *SPI3* is shown in Figure 5. By construction there are no (large) biases between the datasets because 1981–2010 is used as reference period for calculating *SPI3* (Figure A9). The CH2018 multi-model ensemble shows a tendency for slightly positive *SPI3* trends in Northern and Central Europe (however mostly not significant at the 5% significance level) and no tendency in Switzerland and Southern Europe. The observations, in contrast, suggest a decrease of *SPI3* in Southern Europe (significant in one of the observational datasets). COSMO-CLM^2 also shows a significant negative *SPI3* trend in Southern Europe and as well in Central Europe. The fact that there is no significant *SPI3* trend in Switzerland agrees with the CH2018 report, which found no significant trends in the standardized precipitation evapotranspiration index (SPEI, p.43 CH2018 report).

The average number of summer months, during which *SPI3* is lower than -0.5 (mild drought, see e.g., Orlowsky and Seneviratne 2013) shows strong year-to-year variations (Figure 6; note that *SPI3* is based on the monthly values in this case). For Switzerland, the very dry summer 2003 is visible in the observational datasets, and the 2015 drought is mainly observable in Central Europe. For Central and Southern Europe both COSMO-CLM^2 and the

observations show an increasing frequency trend, which is significant in COSMO-CLM[2] in both regions and in the observations in Southern Europe), while the CH2018 multi-model ensemble does not exhibit strong trends. In Northern Europe all datasets show a slight decreasing frequency trend. In Switzerland the observations and COSMO-CLM[2] show a slight (but not significant) increase, while the median of the CH2018 multi-model ensemble shows no signal in the frequency of *SPI3* being lower than -0.5.
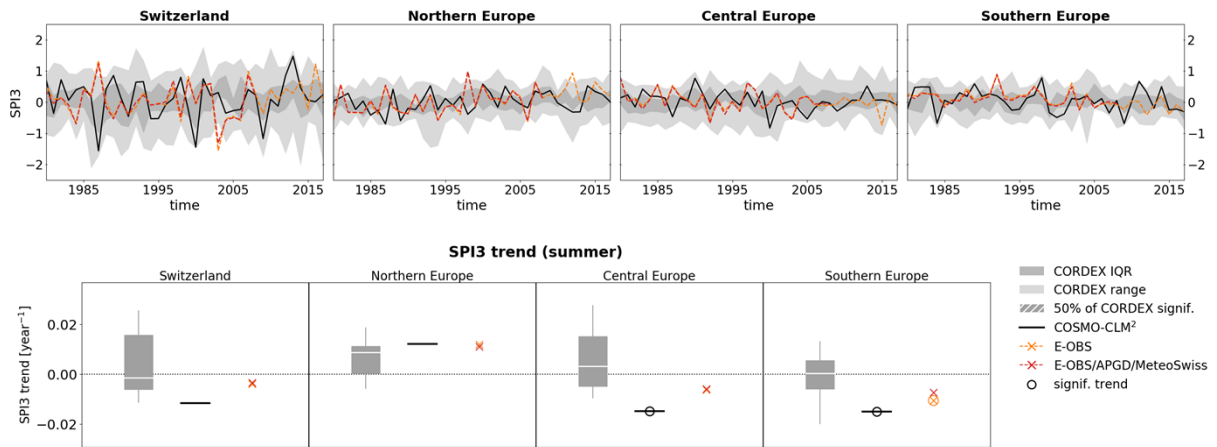

**Figure 5: As in Figure 4 but for the 3-month standardized precipitation index (*SPI3*) averaged over summer.**
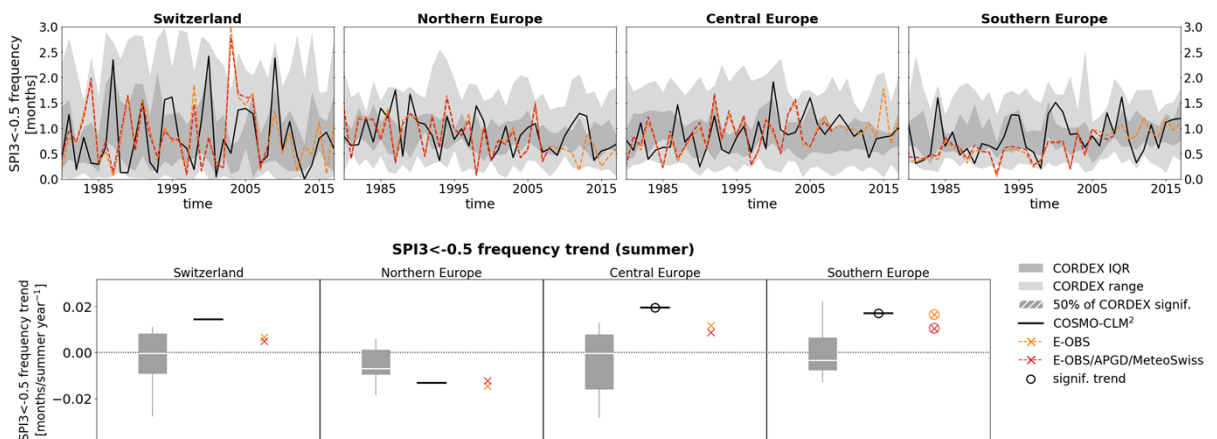
Figure 6: As in Figure 4 but for the average number of summer months, during which *SPI3* is lower than -0.5.

Evapotranspiration in the CH2018 multi-model ensemble and in COSMO-CLM[2] tend to be lower than in the observations, especially in Southern Europe and Switzerland (Figure 7, upper panel; see also Figure A11). However, the different observation-based estimates also often show a large spread, highlighting existing uncertainties in these observational datasets. In Switzerland, both the CH2018 multi-model ensemble and COSMO-CLM[2] exhibit a small positive *E* trend, which is, however, only partly supported by the observations, as they do not agree on the sign of the trend. In Central and Southern Europe, the observations generally have positive *E* trends, while the trends in the CH2018 multi-model ensemble and COSMO-CLM[2] are small on the average (or even negative for COSMO-CLM[2] in Southern Europe). It should be noted that some of the observational datasets (in particular WECANN and GLEAM_v3.2b) only span a short time period and, thus, the trend estimation from these datasets cannot be considered as robust since existing decadal oscillations can influence the estimation.
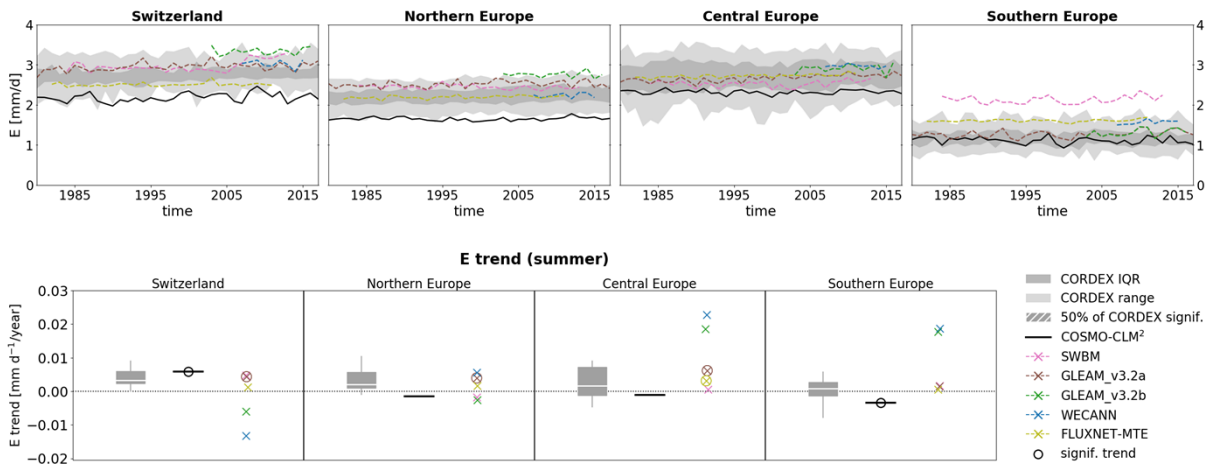
Figure 7: As in Figure 4 but for summer mean evapotranspiration (*E*). Note that the historical estimates for *E* span different and sometimes only short time periods (in particular WECANN and GLEAM_v3.2b). Thus, the trend estimation from these datasets cannot be considered as robust and comparisons between datasets is difficult. Also, significance in the trend is only calculated when at least 15 years of data is available.

For *P-E*, the climate models often exhibit higher values than the observation-based estimates (Figure 8, upper panel; see also Figure A12). The overestimations are especially pronounced in Switzerland and Southern Europe, suggesting that they are connected to the underestimation of *E* by the climate models. The higher variability in Switzerland is most likely due to the lower number of considered grid cells for the area average. In all regions, the observations exhibit no significant observational trends in *P-E*. The CH2018 multi-model ensemble agrees with this pattern, except for Switzerland where some models tend to exhibit negative trends (mostly not significant). The same also applies for COSMO-CLM^2, which has larger negative trends in Switzerland and Central Europe (related to the decrease in summer precipitation in both domains and the increase in *E* in Switzerland).
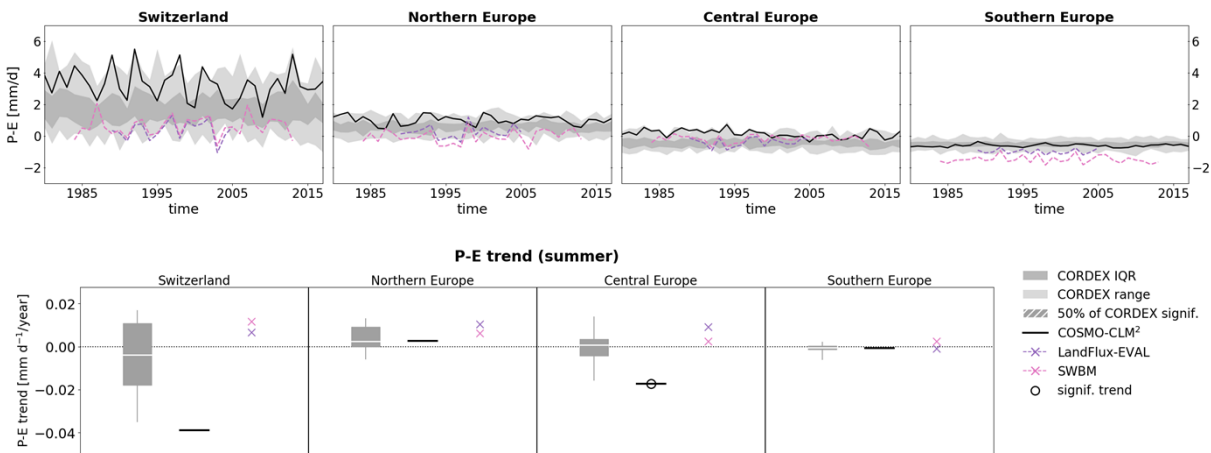
Figure 8: As in Figure 4 but for summer mean of precipitation minus evapotranspiration (*P-E*).

Soil moisture anomalies (*SMA*) in the observations, the CH2018 multi-model ensemble and COSMO-CLM^2 are shown in Figure 9. As for *SPI3*, the mean biases are small, as 1981–2010 is used as reference period for calculating *SMA* (Figure A13). The observational datasets show a decreasing *SMA* trend in Northern and Southern Europe, but they do not agree on the sign of the trend in Central Europe and Switzerland. A reason for this might be that CCI-SM only represents surface soil moisture in the top few centimetres of the soil (Dorigo et al., 2017), while SWBM integrates over deeper soil layers (as it calculates soil moisture based on observed precipitation, temperature and net radiation). The CH2018 multi-model ensemble shows a tendency for negative trends in Southern Europe and Switzerland, which

are, however, mostly not significant. COSMO-CLM² also shows significant negative trends in these two regions. The sign of SWBM trend and the median trend of the CH2018 multi-model ensemble generally agree, which hints to the fact that SWBM soil moisture might be better comparable to climate models as it also considers deeper soil layers. Considering Switzerland there is a pronounced disagreement for *SMA* trends in CHS, with CCI-SM exhibiting significant positive and SWBM showing significant negative trends (Figure A6). The negative SWBM trend in CHS likely reflects the general drying trend in Southern Europe, while the positive CCI-SM trend could reflect increased irrigation (which mostly affects the uppermost soil layers and is not accounted for in SWBM) in Northern Italian grid cells, which are included in the CHS domain and exhibit intensive agriculture and irrigation (see also Figure 23).
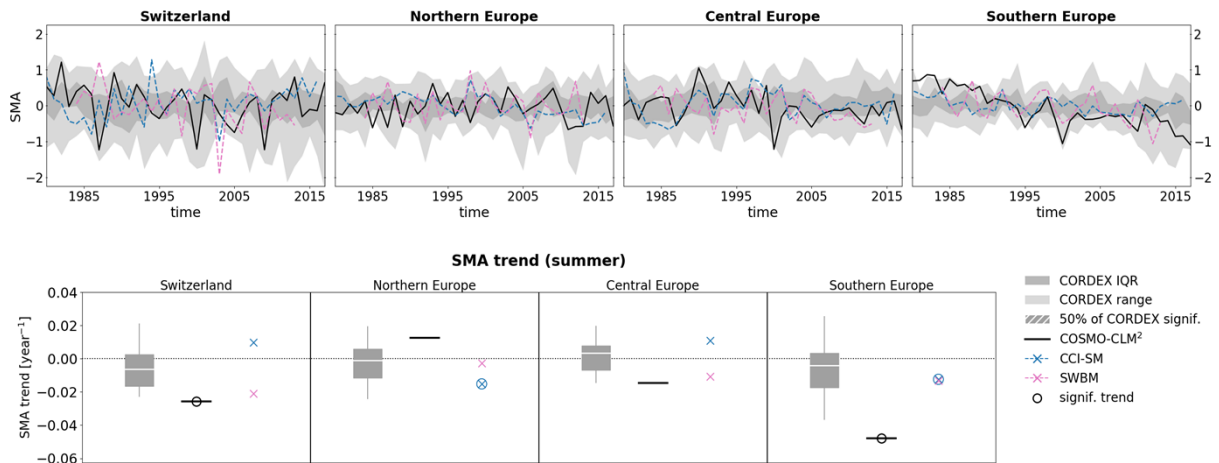
Figure 9: As in Figure 4 but for summer mean soil moisture anomalies (*SMA*).

Standardized runoff anomalies (*SRA*, calculated relative to the reference period 1981–2010) are shown in Figure 10. The CH2018 multi-model ensemble does mostly not exhibit strong trends, while the observations suggest negative *SRA* trends in Switzerland and Southern Europe (although only significant for one observation dataset in Southern Europe) This observed pattern is consistent with previous studies (see e.g., Stahl et al. 2010; Gudmundsson et al. 2017). COSMO-CLM² also exhibits negative trends in Switzerland and Southern Europe, and in addition in Central Europe (significant in Central and Southern Europe).
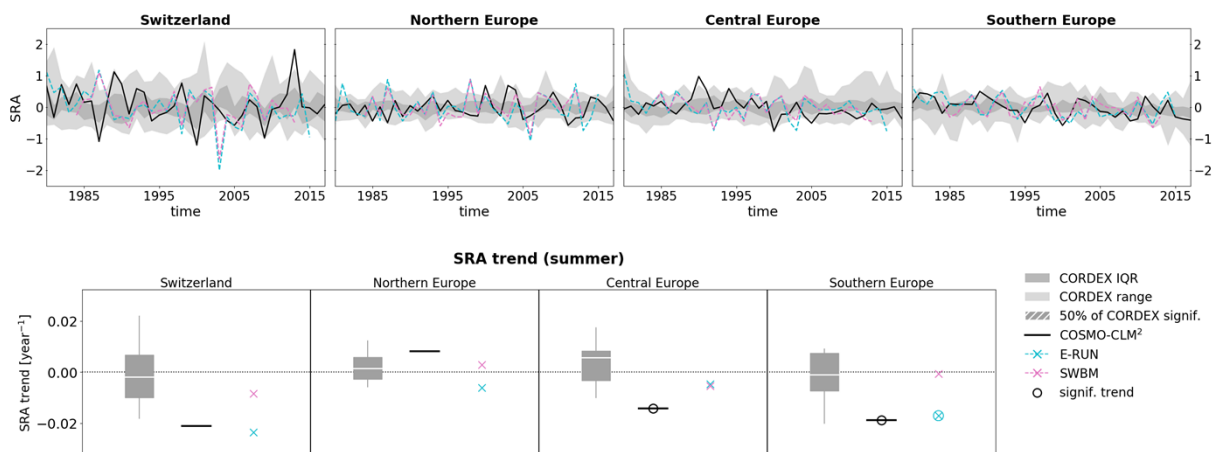
Figure 10: As in Figure 4 but for summer mean surface runoff anomalies (*SRA*).

For most of the assessed drought and water-balance indices, the climate models and the observations generally agree on the historical magnitude and trends. Yet, there are several instances where observations show a significant trend, while there is never a majority of CH2018 multi-model ensemble with significant trends. Additionally, for *E* and *P-E* there is a clear bias between the climate models and the observations, especially in Switzerland and

Southern Europe. The observational datasets often indicate drying trends in Southern Europe. Also, trends in Switzerland go rather towards drying, although the observational trends in Switzerland are not significant. The CH2018 multi-model ensemble on the average shows very small trends for Switzerland, while COSMO-CLM² shows stronger decreases for *P-E, SMA*, and *SRA* in this region.

5.4 Scaling with global mean temperature

The regional future responses of various climate indices often scale with global mean temperature across emission scenarios and thus with accumulated CO_2 emissions (Seneviratne et al., 2016). These functional relationships between global mean temperature and various climate indices from the CMIP5 model ensemble have been implemented into an interactive plotting framework (Wartenburger et al., 2017)[10] that allows to extract regional climate change impacts based on global temperature targets (such as the 2° and 1.5° limits agreed within the 2015 Paris Agreement). For the Mediterranean region, some of the applied drought indices (i.e., *CDD, SPI12, SMA, P-E*) show a distinct scaling with global mean temperature, while for the Central European domain, the changes are insignificant and accompanied by a low signal to noise ratio (Greve et al., 2018; Wartenburger et al., 2017).

This plotting framework has been expanded within Hydro-CH2018 by the more localized EURO-CORDEX simulations from the CH2018 multi-model ensemble. Thereof, we employ all RCM-GCM model chains that provide a transient simulation from 1971–2099 for any of the three emission scenarios RCP2.6, RCP4.5 and RCP8.5 (see CH2018 technical report, Table 4.1 therein).

Results on this smaller regional scale still reveal a quasi-linear scaling of the climate indices with global mean temperature (Figure 11). However, the water balance and drought indices reveal clear differences in these functional relationships between Central Europe and the Alpine and CH2018 sub-domains. For *P-E*, all three domains show a drying tendency in summer, which is amplified in the Alpine and the CH2018 domain Northeastern Switzerland (though with larger inter-model spread). For *SMA* and *SRA*, the signals even switch the direction between the domains. The non-existing trend in *SRA* and the positive trend in *SMA* (i.e., wetting) in Central Europe in fact turn into negative trends for both indices for the Alpine and the Swiss domain in summer.

Thus, the Alpine and CH2018 sub-domains exhibit more pronounced and robust signals in the water balance and drought indices while in the Central European domain, wetting trends in northern part of the domain are mixed with drying trends in the southern part, leading to a dilution of the responses. Switzerland, however, is situated at the dry edge of the large-scale European signals (see also CH2018 technical report), which manifests in clearer responses of the water balance and drought indices. The difference between the domains appears most pronounced for *SMA*, i.e., when storage and pre-conditioning effects are considered.

Regarding differences between 2° and 1.5° global temperature targets, the water balance and drought indices show only non-significant differences between these two targets both for the larger Central European domain as well as for the smaller Alpine and CH2018 Swiss domains.

---

[10] http://drought-heat.ethz.ch/atlas/
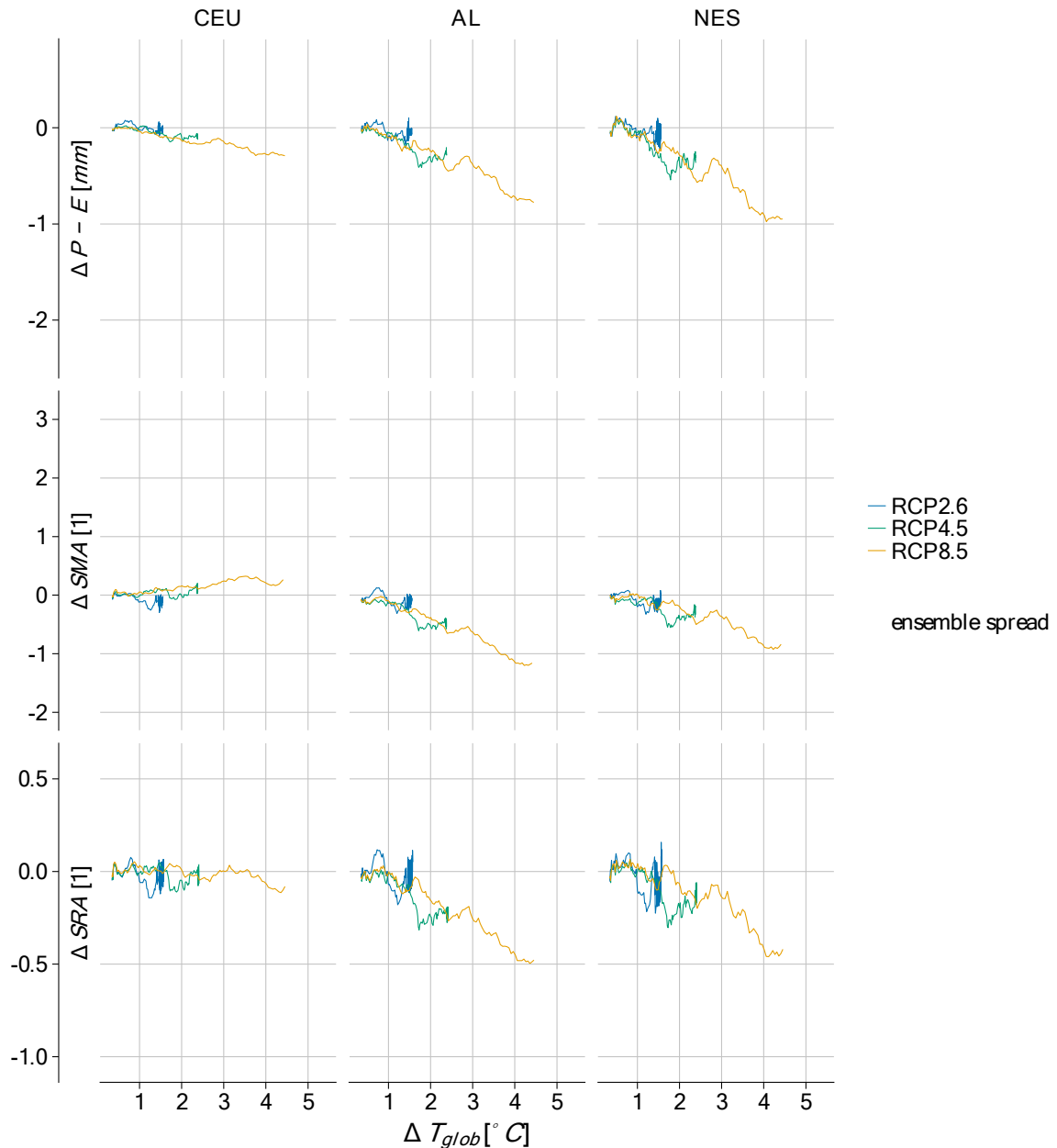
Figure 11: Scaling of the indices *P-E*, *SMA* and *SRA* with global mean temperature in the Central European domain (left column), the larger Alpine region (middle column) and the CH2018 domain Northeastern Switzerland (right column). Summertime changes in the indices are displayed relative to 1971–1990, while the global mean temperature anomaly is adjusted for the warming since the pre-industrial time period (offset of 0.3°C). Plots are based on http://drought-heat.ethz.ch/atlas/.

Lastly, it should be noted that studies indicate differences in climate projections based on RCMs as compared to GCMs (Kjellström et al., 2018; Sørland et al., 2018). The former tend to project a smaller temperature increase than the latter, as well as more precipitation (or less drying). This was hypothesized to be due to discrepant representations of topography, cloud processes, or aerosol forcing in RCMs and GCMs. In addition, the consideration of the plant-physiological CO_2 effect in most GCMs, but generally not in RCMs, may play a key role in explaining this difference (see Section 5.6). At higher CO_2 concentrations, plants close their stomata openings, which can reduce evapotranspiration and result in feedbacks to temperature. This process may account for 67% of the stronger annual maximum temperature increase in GCMs compared to RCMs.

5.5 Temporal future changes

Here, we discuss projections of changes in the hydrological cycle during summer (June, July, August) using the CH2018 multi-model ensemble and two COSMO-CLM^2 simulations: the simulation which takes into account plant-physiological CO_2 effects but does not consider irrigation, and the one that additionally considers irrigation (experiments (2) and (3) listed above). The more specific irrigation effects on the water balance based on COSMO-CLM^2 are presented in Section 5.7. In agreement with CH2018, the 90% and interquartile ranges for the projected seasonal means of the drought and water balance indices are determined empirically from the RCMs. The former is interpreted as a "likely" range, implying at least a 66% probability of reality falling in between. Corresponding projected changes for the five CH2018 Swiss domains are shown in Figure A22 – A28 of the Appendix.

The CH2018 multi-model ensemble projects that *CDD* will substantially increase in Southern Europe, Central Europe, and Switzerland, but only slightly increase in Northern Europe (Figure 12). By the end of the 21st century, *CDD* will extend by about 2-5 days in Switzerland and Central Europe and by about 5-10 days in Southern Europe. For Switzerland, the most pronounced increase in *CDD* is possible for CHS, however with a large uncertainty (Figure A22).
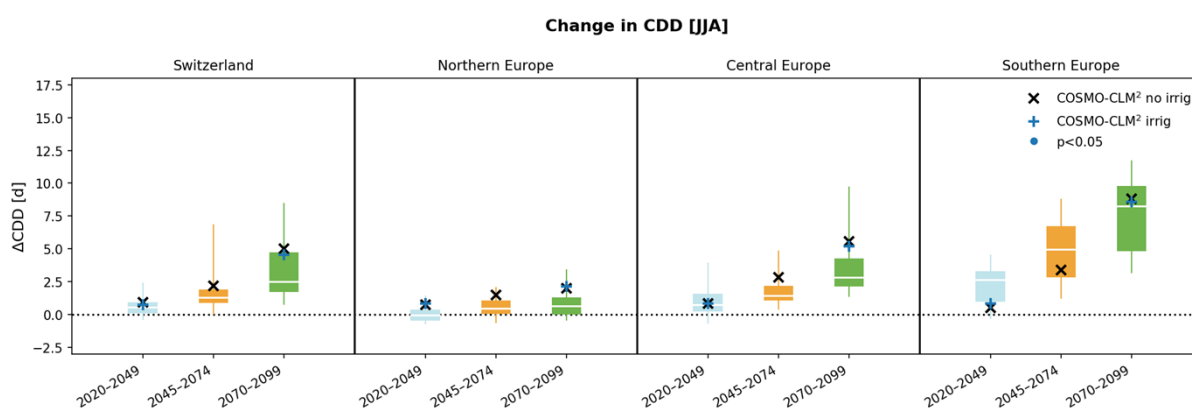
Figure 12: Future changes of the maximum number of consecutive dry days (Δ*CDD*) during summer (June, July, August) in Switzerland, Northern Europe, Central Europe, and Southern Europe during 2020–2049 (light blue boxplots), 2045–2074 (orange boxplots), and 2070–2099 (green boxplots) relative to the 1981–2010 reference period. Black crosses (blue plus signs) indicate the changes in COSMO-CLM^2 without (with) irrigation effects. Blue dots indicate whether the COSMO-CLM^2 irrigation simulation differs significantly from the one without irrigation (based on a Mann-Whitney-U test with a 5% significance level). Note that for the 2045–2074 time period no data for the COSMO-CLM^2 irrigation simulation are available (see Section 5.2.1) The boxplots indicate the distribution of the CH2018 CORDEX models (white lines indicate the median, boxes the interquartile range and whiskers the 5th and 95th percentiles).

SPI3 is projected to slightly increase in Northern Europe, slightly decrease in Central Europe, and strongly decrease in Southern Europe (Figure 13). Switzerland, which combines the signals of the Mediterranean and Central European climate zones, exhibits a wide range of possible *SPI3* changes, ranging from no change to a strong drying comparable to the reduction in Southern Europe. Strong *SPI3* decreases are mostly projected for the Swiss regions CHW, CHS, and CHAW, albeit with substantial uncertainties (Figure A23).

The changes of the number of months during which *SPI3* falls below -0.5 are shown in Figure 14. The frequency slightly decreases in Northern Europe, slightly increases in Central Europe and strongly increases in Southern Europe, consistent with the projected changes of *SPI3* (Figure 13). For Switzerland, the CH2018 multi-model ensemble projects a substantial increase with large uncertainties.
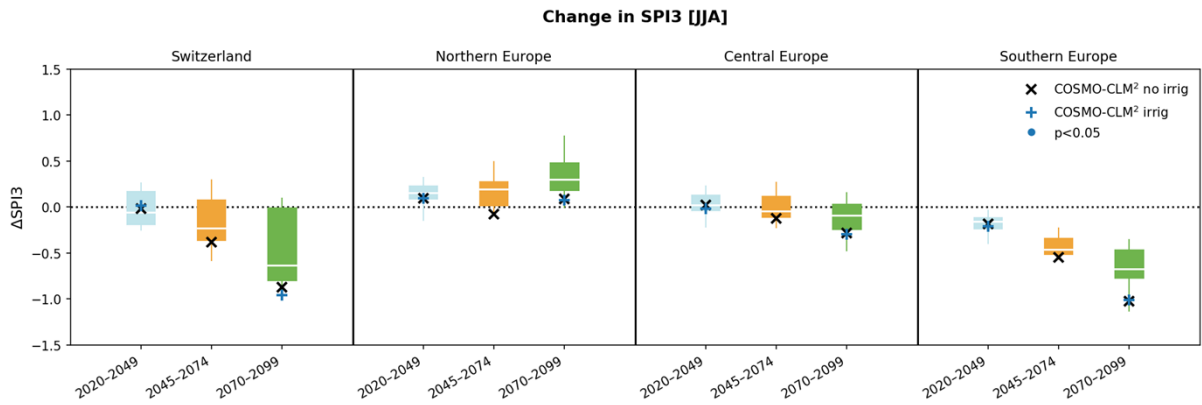
Figure 13: As in Figure 12 but for the 3-month standardized precipitation index (*SPI3*) averaged over summer.
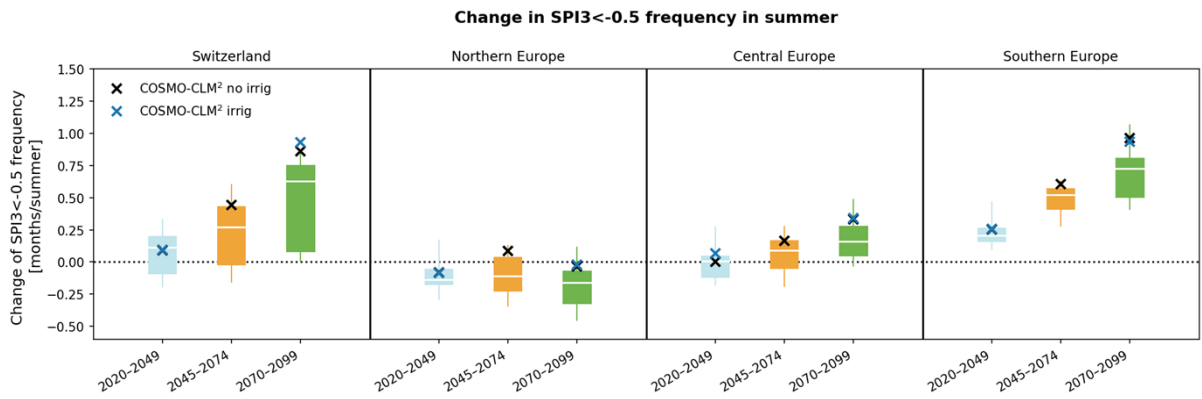
Figure 14: As in Figure 12 but for the average number of summer months, during which *SPI3* is lower than -0.5.

Future evapotranspiration will increase in Switzerland and Northern Europe, will remain mostly constant in Central Europe and will strongly decrease in Southern Europe (Figure 15). In contrast to this, COSMO-CLM² projects that evapotranspiration does not change in Switzerland, while it also projects a decrease in *E* in Northern Europe and Central Europe. This is related to the consideration of plant physiological CO_2 effects in COSMO-CLM² in contrast to the CH2018 multi-model ensemble. The inclusion of plant physiological CO_2 effects strongly affects evapotranspiration projections (and also temperature projections) in Central and Northern Europe (see Section 5.6 for more details).
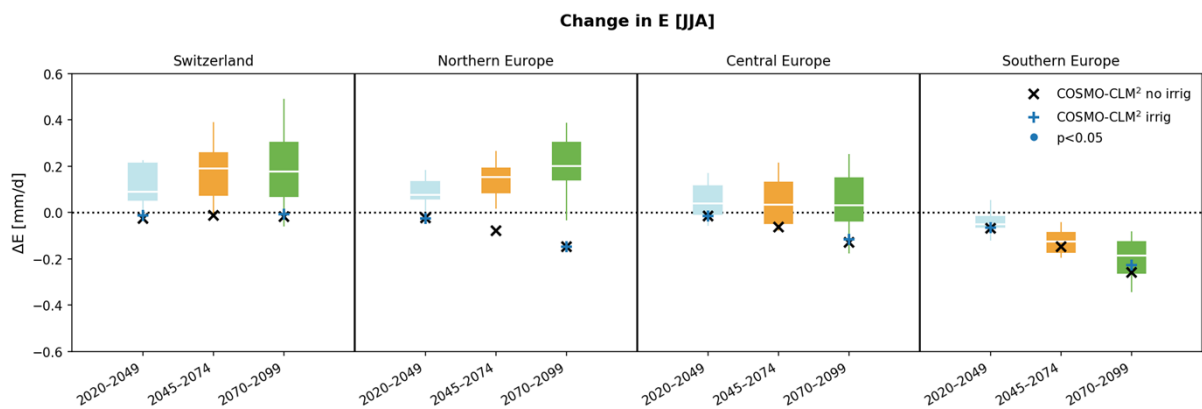
Figure 15: As in Figure 12 but for summer mean evapotranspiration (*E*).

For *P-E*, the CH2018 multi-model ensemble projects a strong decrease in Switzerland and moderate decreases in Northern and Central Europe (Figure 16). In Southern Europe, *P-E* remains almost constant. *P-E* decreases are happening in all Swiss regions, but they are strongest in CHAE and CHAW, suggesting that alpine climate change substantially affects *P-*

E. The strong decrease of *P-E* in Switzerland is both connected to a projected precipitation decrease (Figure 13) and an increase in evapotranspiration (Figure 15).

Change in P-E [JJA]
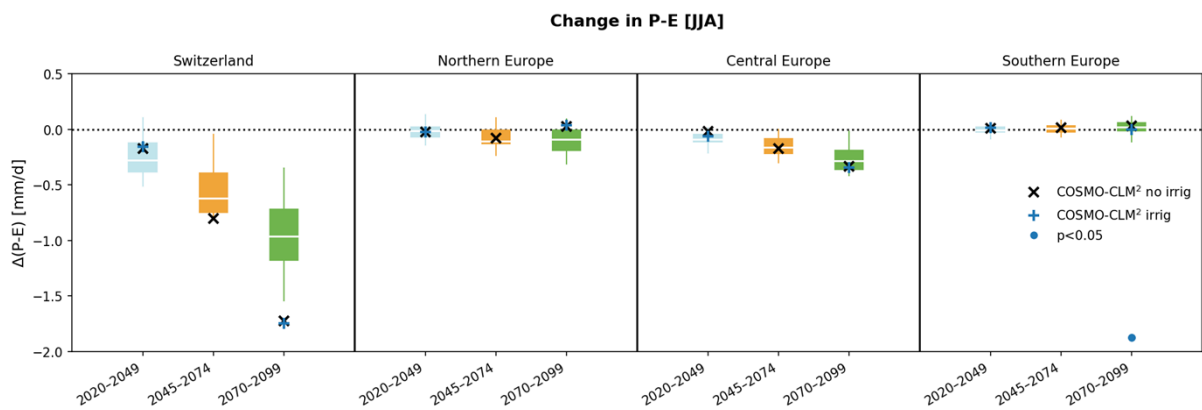
Figure 16: As in Figure 12 but for summer mean of precipitation minus evapotranspiration (*P-E*).

Soil moisture (*SMA*) is projected to decrease in all regions except Central Europe, where trends are only small (Figure 17). Especially in Southern Europe, but also in Switzerland, *SMA* decreases are strong, with some climate models projecting a decrease of 2 to 3 standard deviations. In Switzerland, *SMA* decreases are strongest in the alpine regions CHAE and CHAW, which appears to be related to carry-over effects due to less snow storage and earlier spring snow melt (see also CH2018 technical report, Chapter 6.7 therein).

Change in SMA [JJA]
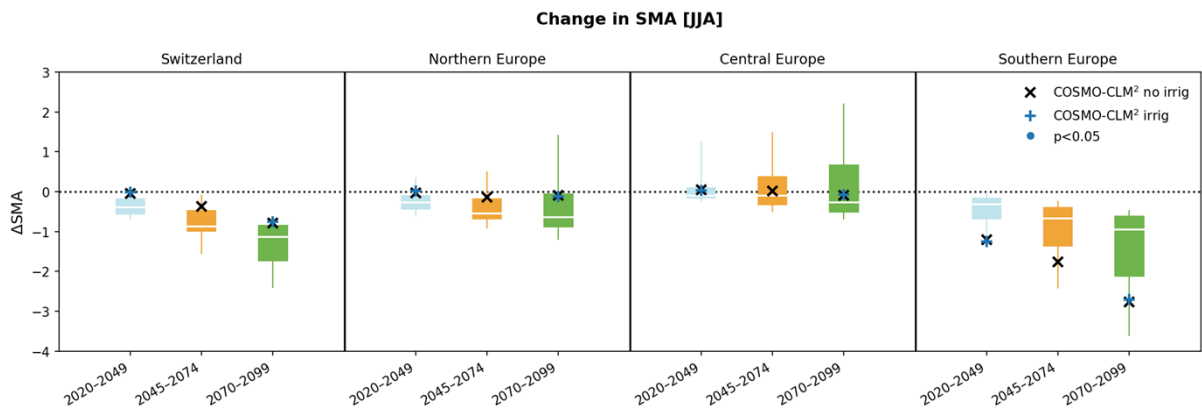
Figure 17: As in Figure 12 but for soil moisture anomalies (*SMA*).

Future changes in runoff (*SRA*) mostly follow the changes of *SMA* with strong decreases in Switzerland and Southern Europe and only slight changes in Northern and Central Europe (Figure 18). *SRA* decrease in Switzerland are especially pronounced in the alpine regions CHAE and CHAW, reflecting again the reduced ice and snow storage in the mountains and earlier spring snow melt.
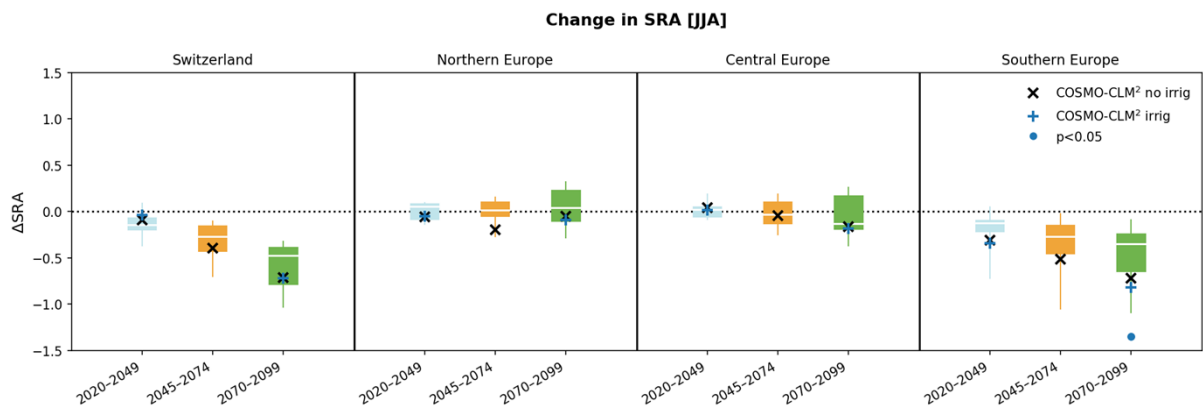
Figure 18: As in Figure 12 but for mean surface runoff anomalies (*SRA*).

Future projections of changes of the hydrological cycle exhibit a strong drying trend in Southern Europe (reflected in all investigated variables but *P-E*) and only slight changes in Central and Northern Europe (with Central Europe having a drying tendency and Northern Europe rather a wetting tendency). Due to the geographical location of Switzerland, it combines both features of Southern and European climate change and, additionally, has some remarked changes in the alpine regions. As a consequence, the projections for Switzerland are often more uncertain (especially for *SPI*, *E*, and *P-E*). The five considered Swiss regions sometimes show diverse trends and local assessments should thus consider the projected evolutions in the single regions (Figure A22 – Figure A28).

5.6 Plant-physiological CO_2 effect on evapotranspiration and impact on temperature extremes

(Based on Schwingshackl et al. 2019)

Increasing atmospheric CO_2 concentrations enhance temperatures on Earth through a stronger absorption of longwave radiation in the atmosphere. In addition to this radiative effect, changing CO_2 concentrations also impact plant physiology (Engineer et al., 2016). At higher CO_2 concentrations plants can increase the fraction of carbon assimilation to transpiration (i.e., the water-use efficiency) by closing pores ('stomata') that are situated on their leaf surface (Keenan et al., 2013; Morison, 1985). Depending on water availability these plant physiological CO_2 responses affect the hydrological cycle in different ways. In water-limited regions, higher water-use efficiency can lead to vegetation greening (Donohue et al., 2013) and a reduction in streamflow (Ukkola et al., 2016). In regions where water is not limited, however, CO_2-enrichment experiments find a decrease of transpiration at elevated CO_2 concentrations for various vegetation types (Bernacchi and VanLoocke, 2015; Donohue et al., 2017).

Most of the GCMs participating in the Coupled Model Intercomparison Project phase 5 (CMIP5) consider plant physiological responses to CO_2 increase (Swann et al., 2016) and show that stomatal adaptation can substantially affect the hydrological cycle (Hong et al., 2018; Lemordant et al., 2018) and even contribute to the amplification of future heat extremes (Lemordant and Gentine, 2019; Skinner et al., 2018). Despite the importance of this process, and in contrast to most GCMs, RCMs generally do not consider plant physiological CO_2 responses. We hypothesize that this systematic discrepancy might be partly responsible for the fact that RCMs predict a smaller temperature increase than GCMs over several European regions (Sørland et al., 2018).

To evaluate differences in future climate projections between GCMs and RCMs, 21 GCM-RCM model chains of EURO-CORDEX are used (see Section 5.2.1). According to the respective model descriptions, none of the RCMs but seven out of the nine driving GCMs consider plant physiological CO_2 responses. To focus on the question of whether the choice of GCM or RCM simulations changes climate projections over the European domain, we compare the 21 RCM simulations to the simulations of the nine driving GCMs. By only using

the driving GCMs we can discriminate any potential effects that would be introduced through an enlargement to the full CMIP5 model ensemble.

The considered GCMs exhibit an amplified future increase of the annual maximum temperature (TXx) compared to the RCMs (violet and blue shadings in Figure 19). The TXx amplification is strongest in central and northern Europe but only small in southern Europe. Additionally, the inter-model spread in both RCMs and GCMs is large in central and northern Europe but narrower in southern Europe. The amplified TXx increase in GCMs in central and northern Europe is consistent with the expectation that plant physiological CO_2 effects on temperature are strongest in regions, which are not water limited (Skinner et al., 2018).
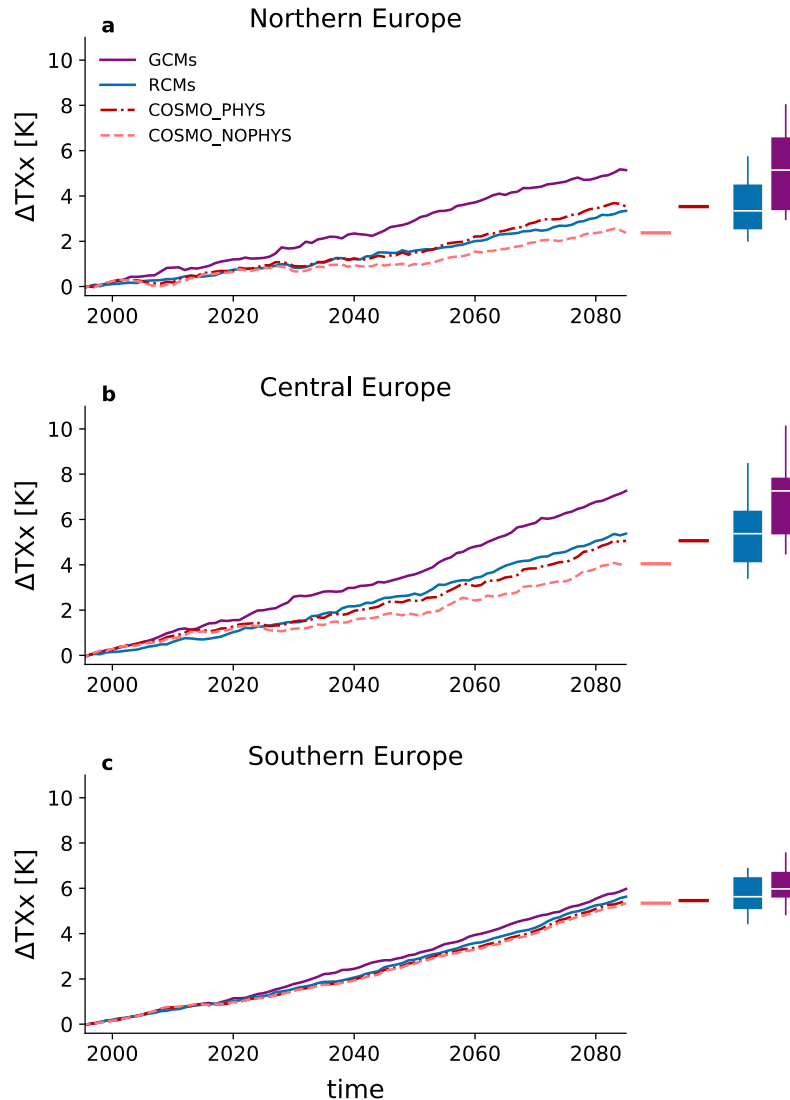
Figure 19: Future projections of annual maximum temperature (TXx). TXx evolution in (a) northern Europe, (b) central Europe, and (c) southern Europe between 1995 and 2085 (30-year moving average) relative to 1981–2010 for RCMs, GCMs, COSMO_PHYS, and COSMO_NOPHYS. Shading for RCMs and GCMs represents the total model range, lines denote the median. The red lines on the right mark the mean ΔTXx during 2070– 2099 for COSMO_PHYS and COSMO_NOPHYS, the box-and-whisker-plots indicate the median (line), interquartile range (boxes) and total range (whiskers) of the ΔTXx distribution in GCMs and RCMs during 2070–2099.

To test the hypothesis that the missing plant physiological CO_2 response in RCMs contributes to the evident GCM-RCM difference, two distinct simulations with a state-of-the-art regional climate model (COSMO-CLM², see Section 5.2.1) are performed. The simulations cover the European domain and range from 1970 to 2099, employing the RCP8.5 scenario (Riahi et al., 2011). One COSMO-CLM² simulation follows the standard

EURO-CORDEX setup and does not include plant physiological responses (hereafter denoted as 'COSMO_NOPHYS'), while the second simulation includes plant physiological responses to rising CO_2 concentrations ('COSMO_PHYS', see Section 5.2.1). Consistent with the amplified TXx increase in GCMs, COSMO_PHYS exhibits a stronger TXx increase compared to COSMO_NOPHYS in central and northern Europe, while in southern Europe the difference is only small (Figure 19). According to the difference between COSMO_PHYS and COSMO_NOPHYS, the contribution of plant physiological responses to the stronger TXx increase in GCMs compared to RCMs is around 81% in northern and 73% in central Europe (contribution to the median increase of all paired 21 GCM-RCM combinations). Note that the TXx signal in COSMO-CLM² is on the lower side compared to the RCM ensemble. We anticipate that this is not connected to the CLM land surface scheme, but more likely due to the fact that the driving GCM (MPI-ESM-LR) used to force COSMO-CLM² shows a lower temperature change signal than many of the other GCMs in the EURO-CORDEX ensemble (Kjellström et al., 2018; Sørland et al., 2018).
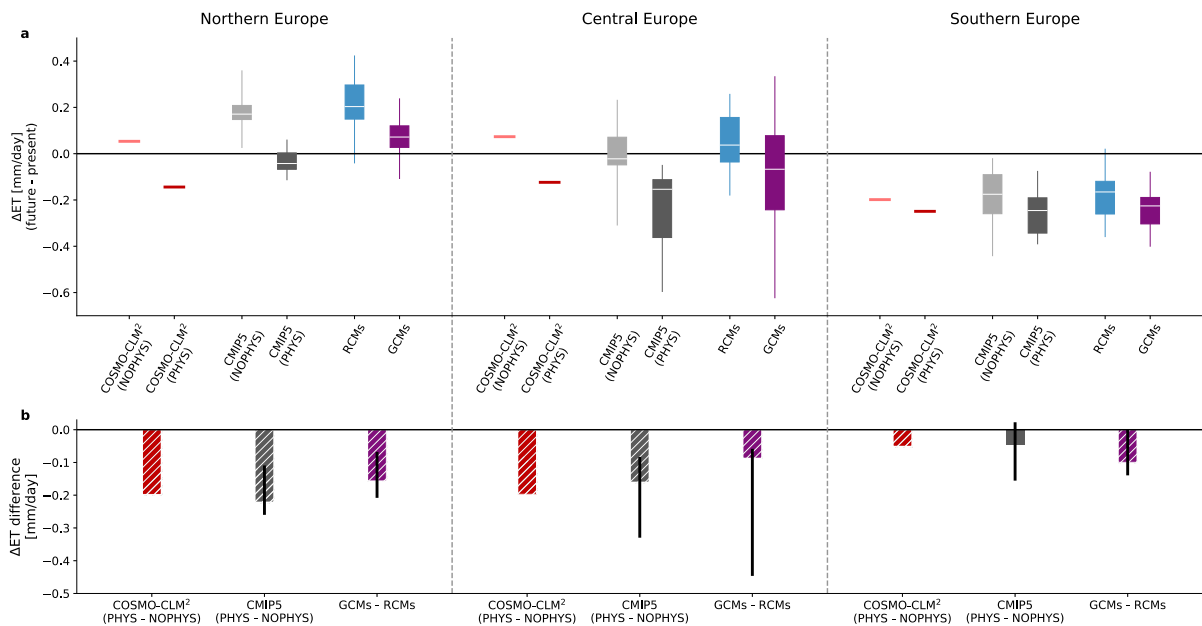
Figure 20: Change in summer evapotranspiration (ET) due to climate change and plant physiological CO_2 effects in three European regions. (a) Mean evapotranspiration changes (ΔET) between 1981–2010 and 2070–2099 for COSMO_NOPHYS (light red), COSMO_PHYS (red), RCMs (blue, number of models N=21), and GCMs (violet, N=9) and at 2070–2099 CO_2 concentrations relative to 1981–2010 CO_2 concentrations for CMIP5_NOPHYS (light grey, N=8) and CMIP5_PHYS (dark grey, N=8). The box-and-whisker-plots indicate the median (line), interquartile range (boxes), and total range (whiskers) of the ΔET distribution across climate models. (b) Difference of evapotranspiration changes (ΔET difference) between the PHYS and NOPHYS simulations of COSMO-CLM² and the CMIP5 models (median difference, N=8) as well as the median difference of ΔET between the GCMs and RCMs (considering each RCM and subtracting its ΔET from the ΔET in the respective driving GCM, N=21). Black whiskers indicate the interquartile range and hatching denotes significant differences at the 5% level (calculated over 30 years for COSMO-CLM² and over the different models for the CMIP5 models and the GCM-RCM difference; see Schwingshackl et al. 2018 for details).

The amplified TXx increase in COSMO_PHYS compared to COSMO_NOPHYS can be attributed to the stomatal response to elevated CO_2 concentrations in COSMO_PHYS. Smaller stomata openings lead to reduced evapotranspiration (ET), which affects atmospheric temperatures in two ways. Reduced evapotranspiration induces an increase of the fraction of net radiation that is converted to sensible heat flux, causing a stronger heating of near-surface air and affecting, in particular, extreme temperatures (Miralles et al., 2014b; Perkins, 2015). Moreover, reduced evapotranspiration can induce cloud cover reductions,

which leads to higher temperatures through enhanced incoming shortwave radiation. Indeed, future evapotranspiration in COSMO_PHYS is significantly reduced compared to COSMO_NOPHYS (Figure 20). Especially in central and northern Europe the evapotranspiration reduction is substantial (-0.20 mm/day), while in southern Europe it is only small (-0.05 mm/day). The evapotranspiration difference between COSMO_PHYS and COSMO_NOPHYS is composed by a substantial reduction in transpiration and a slight increase in bare soil evaporation (Supplementary Figure 2 of Schwingshackl et al. 2019). The evaporation increase is likely a direct effect of the lower transpiration, which leaves more water in the soil for evaporation. Although the two effects compensate in some regions (particularly in southern and eastern Europe), the dominating signal over central and northern Europe is a considerable decrease of evapotranspiration (Figure 20).

The evapotranspiration reduction in COSMO_PHYS agrees well with estimates from dedicated CMIP5 simulations, which aim at quantifying climate effects of plant physiological CO_2 responses (see Methods). The median evapotranspiration reduction due to plant physiological responses in the CMIP5 models (CMIP5_PHYS minus CMIP5_NOPHYS) is similar to the reduction in COSMO-CLM[2] in northern, southern and, a bit less pronounced, in central Europe (Figure 20). The evapotranspiration effect in COSMO-CLM[2] can also be compared to evapotranspiration measurements from CO_2-enrichment experiments, in which plants are exposed to elevated CO_2 concentrations. The evapotranspiration sensitivity to atmospheric CO_2 increase in COSMO-CLM[2] (ranging from -1.1%/100 ppm to -2.8%/100 ppm) agrees well with median estimates from various experiments in grasslands (-2.6%/100 ppm, number of observations N=7), crops (-2.8%/100 ppm, N=19), and forests (-1.0%/100 ppm, N=24), as shown in Figure 21. The evapotranspiration reduction induced by plant physiological CO_2 responses in COSMO-CLM[2] is thus well in line with both the CMIP5 simulations on plant physiological forcing and the observation-based estimates.
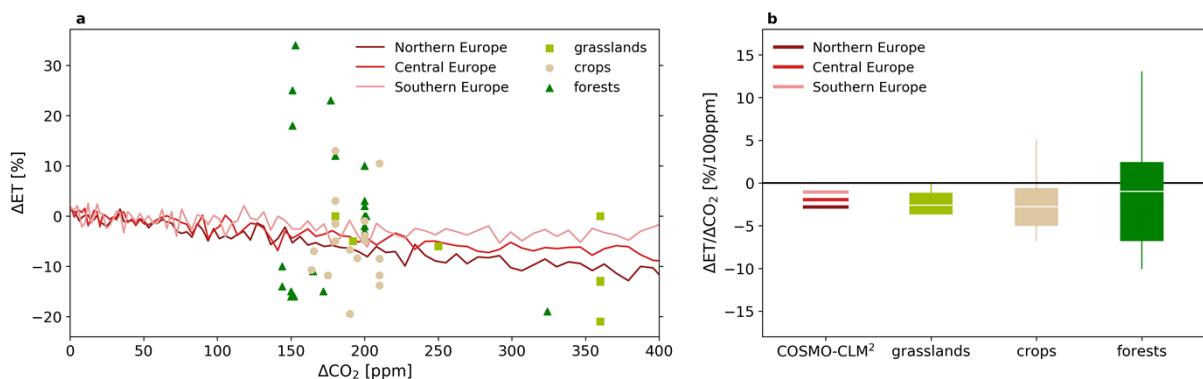
Figure 21: Effect of elevated CO_2 on evapotranspiration (ET) in observations and in COSMO-CLM2. (a) evapotranspiration difference between elevated and ambient CO_2 conditions (given as percentage change with respect to ambient conditions) as function of ΔCO_2 (elevated minus ambient CO_2 concentrations) in different CO_2-enrichment experiments (markers) and evapotranspiration difference between the COSMO-CLM2 PHYS and NOPHYS simulations (given as percentage change with respect to the 1981–2010 average of PHYS) as function of CO_2 change (with respect to the 1981–2010 average) in northern, central, and southern Europe (lines). (b) Sensitivity of evapotranspiration to CO_2 changes in COSMO-CLM[2] and in observations. For COSMO-CLM[2] the sensitivity is estimated as linear fit between ΔET and ΔCO_2 during 1970–2099. For the observations, lines in the box-and-whisker-plots represent the median, boxes the interquartile range, and whiskers the 5th and 95th percentiles.

Consistent with plant physiological responses, the nine driving GCMs of the 21 GCM-RCM model chains generally project a reduced evapotranspiration change compared to RCMs at the end of the 21st century (Figure 20). The difference between GCMs and RCMs is largest in northern Europe, where also COSMO-CLM[2] and the CMIP5 models show strong evapotranspiration reductions due to plant physiological effects, and relatively small in

southern Europe. In central Europe, the median GCM-RCM difference is smaller than in northern Europe, but the uncertainty is high and the distribution strongly skewed towards negative values. This large uncertainty of the evapotranspiration difference between GCMs and RCMs emerges from a large spread of the GCMs (Supplementary Figure 6 of Schwingshackl et al. 2018), which is consistent with results of a recent study (Vogel et al., 2018). When only using the GCM-RCM model chains, in which GCMs consider plant physiological CO_2 responses, evapotranspiration reductions in northern and southern Europe remain robust, but vary considerably in central Europe. Both the evapotranspiration reductions caused by plant physiological CO_2 responses and the evapotranspiration difference between RCMs and GCMs reveal a north-south gradient with strong evapotranspiration reductions in northern and small decreases in southern Europe, suggesting that a large part of the evapotranspiration difference between GCMs and RCMs can be explained by plant physiological responses. The respective evapotranspiration reductions are also consistent with the amplified TXx increase in GCMs compared to RCMs in northern and central Europe (Figure 19), indicating that a considerable percentage of the TXx difference between GCMs and RCMs is indeed due to plant physiological CO_2 responses.

Besides extreme temperatures, plant physiological responses also affect mean temperatures, albeit to a smaller degree (Supplementary Figure 4 of Schwingshackl et al. 2018). Land temperatures averaged over the European domain are about 0.38 K higher during summer (June, July, August) in COSMO_PHYS than COSMO_NOPHYS and mean annual temperatures are elevated by about 0.15 K. The pronounced seasonal cycle of the plant physiological CO_2 effects on evapotranspiration and temperature (Supplementary Figure 5 of Schwingshackl et al. 2018) reflects their importance during the vegetation period. Subtracting the temperature effect stemming from plant physiological responses (estimated by COSMO-CLM[2]) from the temperature bias between GCMs and RCMs, which also shows a pronounced seasonal cycle, yields a much more uniform temperature difference in the course of the year (Supplementary Figure 5 of Schwingshackl et al. 2018). Averaged over the European domain the remaining bias is about 0.25 K.

Besides plant physiological CO_2 responses, GCMs and RCMs also exhibit differences related to the representation of topography, cloud processes, and aerosol forcing (Giorgi and Gao, 2018; Sørland et al., 2018). In particular, the discrepant aerosol trends have recently been discussed as possible cause for divergent GCM and RCM climate projections (Bartók et al., 2017; Giorgi and Gao, 2018; Nabat et al., 2016; Sørland et al., 2018). The emission scenario RCP8.5 used in the GCM, RCM, and COSMO-CLM[2] simulations project a strong aerosol reduction over Europe until 2100 (IPCC, 2013; Riahi et al., 2011). While all GCMs incorporate this trend, aerosols in the RCMs used in this study (including COSMO-CLM[2]) are usually prescribed as climatological values without any long-term trends (Giorgi and Gao, 2018). Especially over Europe, reduced aerosol loads contribute an important fraction to the future radiative forcing in GCMs (Westervelt et al., 2015) but not in RCMs (Giorgi and Gao, 2018). A model study with one RCM estimated a temperature increase of 0.3 K over Europe when using RCP8.5 aerosol trends instead of constant aerosol concentrations (Nabat et al., 2016), which is consistent with the 0.25 K temperature bias not explained by plant physiological CO_2 responses. While aerosol radiative forcing is projected to increase mostly in the Mediterranean area and central Europe (IPCC, 2013), the evapotranspiration and TXx differences between GCMs and RCMs are highest in central and northern Europe but only small in southern Europe. This pattern agrees much better with the expected effects of plant physiological CO_2 responses (see Figure 20) than with aerosol effects, suggesting that plant physiology is likely the largest contributor to the TXx amplification in GCMs compared to RCMs in large parts of Europe.
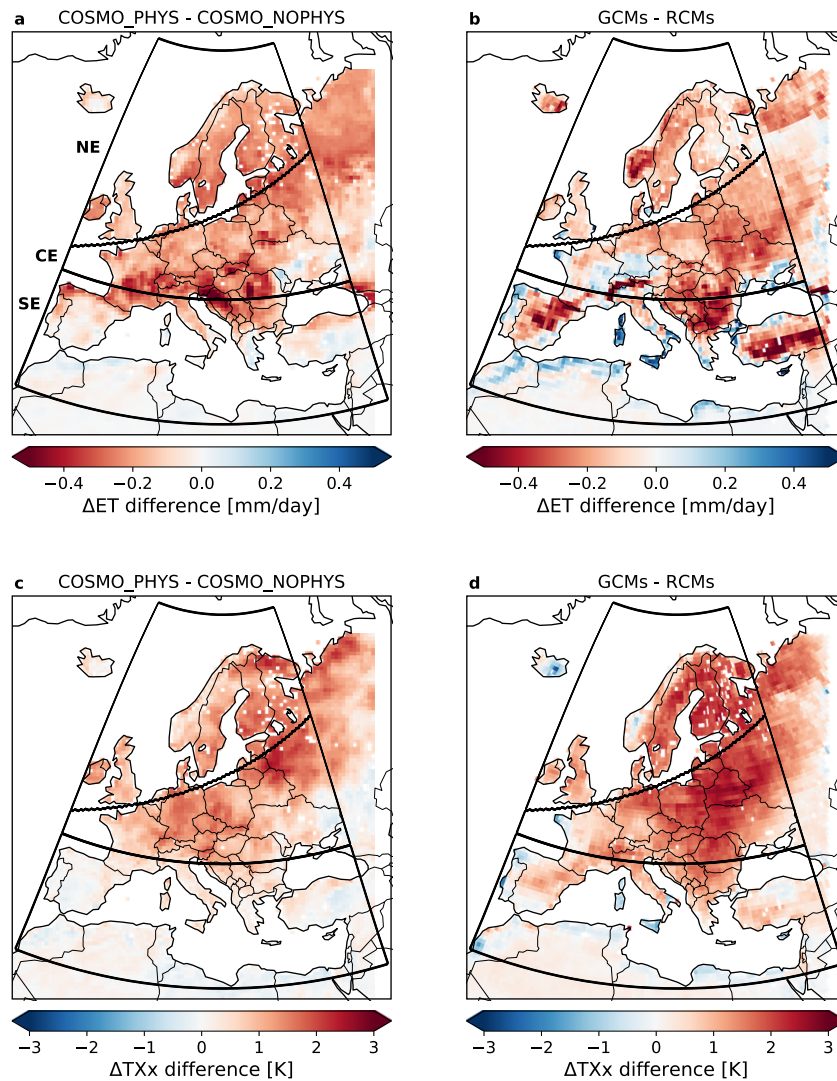
Figure 22: Plant physiological CO$_2$ responses in COSMO-CLM^2 and differences between GCMs and RCMs for summer mean evapotranspiration (ET) and annual maximum temperature (TXx). (a, b) Difference of the future minus present evapotranspiration changes ($\triangle$ET difference) and (c, d) difference of the future minus present TXx changes ($\triangle$TXx difference). Panels a and c show the difference between COSMO_PHYS and COSMO_NOPHYS, panels b and d show the median GCM-RCM difference (calculated for each RCM and its driving GCM, N=21). The evapotranspiration and TXx changes ($\triangle$ET and $\triangle$TXx) of the individual model simulations are calculated as mean changes between 1981–2010 and 2070–2099. Black frames indicate the three study regions southern Europe (SE), central Europe (CE), and northern Europe (NE).

The geographical patterns of evapotranspiration and TXx differences between COSMO_PHYS and COSMO_NOPHYS and between the GCMs and RCMs are shown in Figure 22. In COSMO-CLM^2 the evapotranspiration reduction due to plant physiological CO$_2$ responses is high almost everywhere in central and northern Europe. The strongest effects occur in a band that spans from Southern France to the Black Sea. The evapotranspiration differences between GCMs and RCMs generally agree with this pattern (pattern correlation of 0.37; Spearman's rank correlation, p<0.001) and also reveal high values in eastern and northern Europe. Over topographically complex terrain (such as the Pyrenees, the Alps, Anatolia, or the Scandinavian Mountains) the evapotranspiration differences between GCMs and RCMs are especially pronounced, which might be due to the better spatial resolution of RCMs rather than to plant physiological CO$_2$ responses. The TXx patterns generally follow the patterns of decreased ET, with high values occurring especially in central and eastern to northeastern Europe. While evapotranspiration is more connected to stationary vegetation

processes, for the occurrence of TXx also air advection plays a role. Consequently, the TXx patterns are more widespread with respect to the evapotranspiration patterns. The high pattern correlation of 0.78 (Spearman's rank correlation, $p<0.001$) between the TXx maps of COSMO-CLM^2 and the GCM-RCM maps highlights again the close connection between the plant physiological effects on TXx estimated with COSMO-CLM^2 and the TXx difference between GCMs and RCMs.

The geographical patterns of the evapotranspiration differences (Figure 20 and Figure 22) are in line with the expected evapotranspiration reductions in non-water-limited regions such as central and northern Europe (Bernacchi and VanLoocke, 2015; Donohue et al., 2013), while evapotranspiration decreases are lower or negligible in water-limited regions like southern Europe (Fatichi et al., 2016; Skinner et al., 2018). Summer transpiration in southern Europe is already low in the present (Supplementary Figure 2 of Schwingshackl et al. 2019) and all model sets (COSMO-CLM^2, CMIP5, RCMs, and GCMs) project a net evapotranspiration decrease in the future (see Figure 20, upper right panel). Including plant physiological CO$_2$ effects in COSMO-CLM^2 and CMIP5 only leads to a slight additional evapotranspiration reduction, suggesting that water limitations rather than stomatal effects are the dominating factor for future evapotranspiration evolution in southern Europe.

In water-limited regions, water savings due to reduced evapotranspiration can also extend the growing season (Reyes-Fox et al., 2014). Moreover, increasing CO$_2$ generally leads to an evapotranspiration decrease in undisturbed vegetation, while it induces greening in disturbed (not full grown or damaged) vegetation, which counteracts the evapotranspiration reduction and can even cause an enhancement of evapotranspiration (Donohue et al., 2017). COSMO-CLM^2, which is used in this study, does not consider vegetation dynamics. Instead, leaf area index is prescribed as climatology with no long-term changes throughout the simulation period and the effects of vegetation disturbance and growing season changes are thus not considered. While vegetation disturbance effects might impact the results of this study, possible extensions of the growing season should be less important as TXx typically occurs during summer.

The study highlights the need to include plant physiological CO$_2$ responses in other RCMs in order to provide unbiased regional climate projections that are physically consistent with the driving GCMs. Given the importance of RCM projections in providing information for impact studies and the design of adaptation plans (Gutowski Jr. et al., 2016), it is crucial that RCMs reflect the most recent advances in our understanding of land-atmosphere interactions.

5.7 Effects of irrigation on water cycle and resources

Using dedicated COSMO-CLM^2 simulations (experiment (3) compared to experiment (1) as listed above), we assess how irrigation of agricultural crops affects projected changes of the hydrological cycle (as represented by the applied drought and water balance indices), as well as how simulated irrigation demands change from present to future climate conditions. The irrigation amount in COSMO-CLM^2 is simulated dynamically for the fraction of the crop area being irrigated as prescribed from the present-day distribution of area equipped for irrigation (Section 5.2.1).

Under both present and future climate conditions, irrigation is mostly limited to Southern and Central Europe (Figure 23, see also Figure A29 for a zoom on the Alpine area). Areas with substantial irrigation amounts are the Iberian Peninsula, Italy, the regions around the Black Sea and the Aegean, and the surroundings of the Nile. Future projections of irrigation amounts show that the regions where irrigation is important do not shift much, but within these regions and in surrounding areas the irrigation intensity strongly increases (Figure 23c). Moreover, it is worth noticing that there are no regions, where irrigation is projected to decrease.
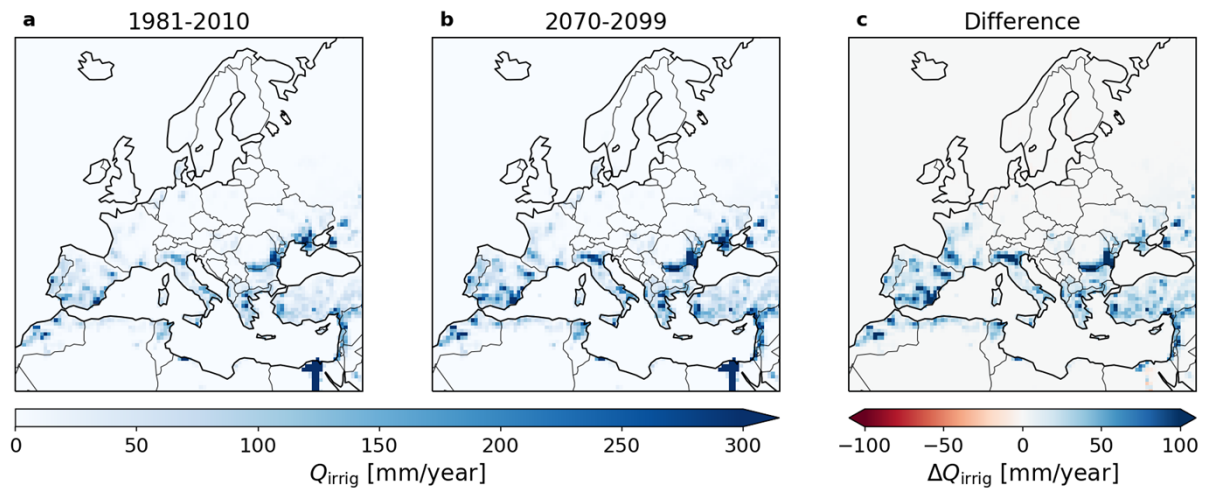
Figure 23: Yearly irrigation amount in COSMO-CLM² during (a) 1981–2010 and (b) 2070–2099 and (c) the irrigation difference between the two time periods.

Figure 24 shows the average irrigation amounts per year in the different regions considered in this report, both for present and 2070–2099 climate conditions. The climate-related irrigation demand reveals high amounts in Southern Europe and moderate amounts in Central Europe and Switzerland. Among the Swiss regions especially CHS shows substantial irrigation amounts (see also Figure A29). For Switzerland and CHS, the irrigation demand is projected to double until the end of the century. Note that the high values in CHS might partly be caused by grid cells of the Po Valley included in this region, where irrigation is particularly high (Figure 23 and A29). All the other Swiss regions only exhibit negligible irrigation amounts.
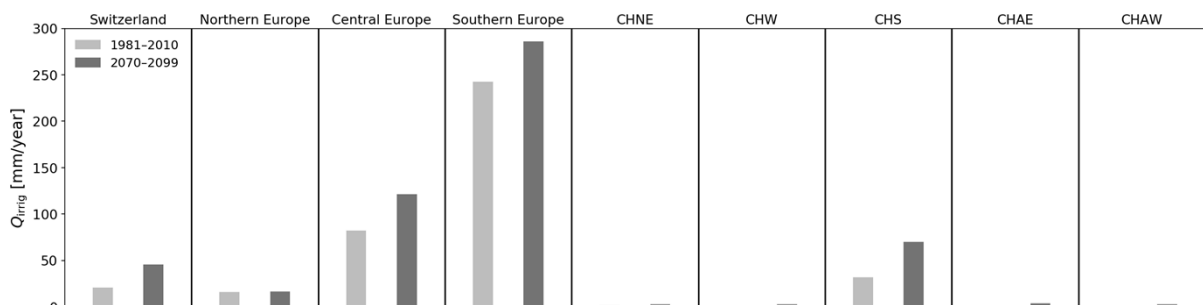
Figure 24: Yearly irrigation amount in COSMO-CLM² in the nine investigated regions during 1981–2010 and 2070–2099 (values representative for irrigated crop areas).

Including irrigation effects in COSMO-CLM² only leads to minor impacts on the future changes of the considered drought and water balance indices (Figure 12 – Figure 18). Significant changes are only evident in Southern Europe, where *P-E* and *SRA* significantly decrease in the latest scenario period (Figure 16 and Figure 18). The reduction of *SRA* is probably connected to the fact that the water for irrigation in COSMO-CLM² is taken from the runoff component, automatically reducing *SRA*. Besides these significant decreases, including irrigation leads to slight (but not significant) reductions in *CDD* and *SRA* and slight increases in *E*. In the Swiss regions CHS and CHAW irrigation further leads to a (non-significant) reduction in *SPI3* (Figure A23). The effect of irrigation on the investigated drought and water balance indices is overall only minor compared to climate change effects and, especially in Switzerland, the hydrological cycle is not much affected.

6   Take-Home Messages

- In response to strong warming, Switzerland is expected to experience a reduction in wet days and a tendency toward longer dry spells (meteorological drought) in summer by the end of the century. The associated increase in evaporative demand is further projected to lead to more pronounced agricultural droughts (drier soils).
- The extent of the projected summer drying, however, remains uncertain (both insignificant and very strong changes cannot be excluded). This is also due to the location of Switzerland in between southern Europe that is projected to experience a severe increase in drought risk, and northern Europe that is expected to experience a winter wetting.
- While the applied drought and water balance indices compare reasonably well with observed indices, process representation in the regional climate models used for the scenario assessment contribute to the reported uncertainties in the CH2018 projections.
- Namely the representation of plant-physiological CO_2 effects may contribute to a reduction in evapotranspiration in Central and Northern Europe and consequent feedbacks on (extreme) temperatures.
- Simulated irrigation demand is projected to increase twofold in Switzerland although feedbacks on the hydrological cycle are generally very small and mostly limited to Southern Europe and the Southern part of Switzerland.

7   Research gaps and open questions

Land use change is potentially an additional important local driver of hydrological change in addition to climate. Simulations with two different versions of the CLM land surface model (Figure 25) indicate however large uncertainties in the evapotranspiration response to land cover conversions at different altitude levels in Switzerland. This thus strongly limits our current predictive capacity to anticipate the hydrological outcome of land cover change in the Alpine context. Progress has been made in understanding and improving evapotranspiration's sensitivity to land cover change at the global scale thanks to the use of new observations (Meier et al., 2018), but understanding these processes in the Alpine context under strong elevation gradients and an associated lack of observational data still remains a research gap.

Red: CLM5.0 – BHS Blue: CLM4.5 – PLUS In units of [mm/d]	Below 1000 m		Above 1000 m	
	DJF	JJA	DJF	JJA
Open land to Needleleaf	*0.17 ± 0.05* *0.26 ± 0.11*	*-0.95 ± 0.26* *-0.06 ± 0.19*	*0.21 ± 0.07* *0.38 ± 0.16*	*-0.49 ± 0.30* *-0.13 ± 0.09*
Needleleaf to broadleaf	*-0.15 ± 0.04* *-0.04 ± 0.08*	*0.65 ± 0.18* *0.06 ± 0.04*	*-0.15 ± 0.04* *-0.06 ± 0.06*	*0.35 ± 0.29* *-0.02 ± 0.07*
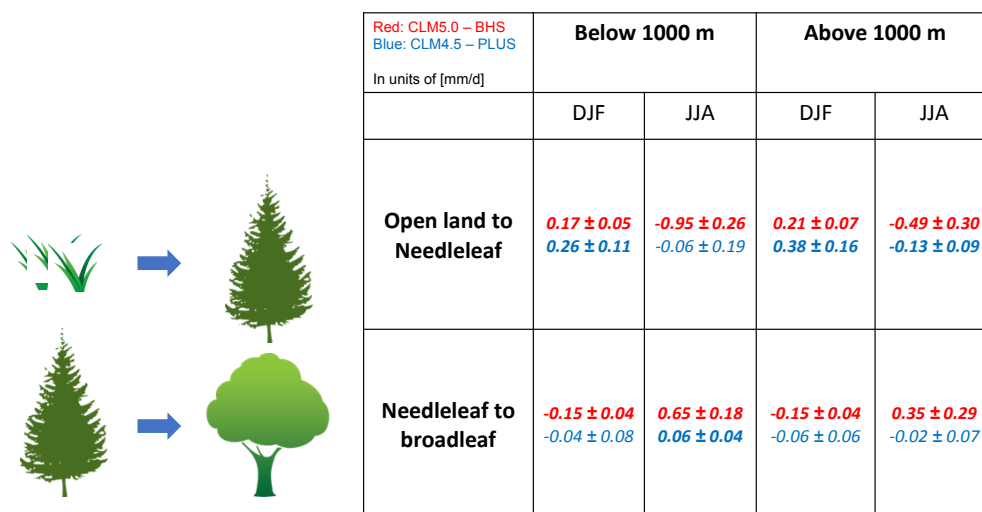
Figure 25: Local evapotranspiration changes induced by land cover transitions at different altitudes in Switzerland as simulated by two versions of the CLM land surface model.

Uncertainties also exist concerning the role of increasing CO_2 on stomatal conductance and canopy scale transpiration (Schwingshackl et al., 2019). Our simulation results indicate that this effect is essential to include in hydrological projections, however results from other models would help assess the robustness of this finding. In addition, evaluating the realism

of modelling results using observationally-based studies should be an essential focus of future studies in this filed.

Concerning the importance of irrigation, it is important to note that our experiments explored only the effect of a changing climate on future irrigation demand (and associated climate feedbacks) assuming constant socio-economic conditions in the future. We acknowledge however that future socio-economical changes (e.g. changes in population and land use) will be an essential driver of future irrigation demand along with climate change (Haddeland et al., 2014). Assessing such socio-economical changes was beyond the scope of this report but consideration of both climatic and socio-economic changes is a research gap that should receive more attention in order to provide more policy-relevant information for decision-making.

Overall, the analysis of climate model simulations suggest that anthropogenic climate change will trigger a systematic summer drying in Switzerland through a reduction in summer precipitation and an increase in evapotranspiration. As terrestrial water systems are critically dependent on these atmospheric boundary conditions the subsequent decrease in summer soil moisture and runoff comes as no surprise. However, while the joint assessment of observed and simulated change indicates some consistency throughout the past decades it remains to-date unclear whether anthropogenic climate change has already altered water resources at the national scale. To tackle this question, climate change detection and attribution techniques have to be employed. These methods are designed to test the hypothesis that the influence of human greenhouse gas emissions, as simulated by climate models, is visible in the observed records while accounting for natural climate variability.

Besides systematic shifts in the mean land water balance, the overall drying tendency in summer does also imply an increased likelihood of soil moisture and hydrological droughts. In this context, the recent occurrence of exceptionally dry summers (2003, 2015, 2018) raises the question whether anthropogenic climate change has contributed to the occurrence of these extreme events. This question can be addressed through the use of extreme event attribution techniques that are designed to deliver quantitative evidence on how human emissions have changed the occurrence probability of climatic extreme events.

8 Concluding remarks and recommendations

The quantitative basis of this report is the analysis of evapotranspiration, soil moisture and drought indices at larger spatial and temporal scales. While this large-scale focus allows to increase the robustness and facilitates a generalization of the results, they cannot be used to infer local-scale climate impacts. To this end detailed case studies, focusing on how atmospheric boundary conditions are impacting terrestrial water availability at the local scale can be employed if care is taken to account for both model uncertainty and natural climate variability in the projections of future climatic conditions. Moreover, the availability of reference observations of soil moisture and evapotranspiration to evaluate process implementation in the models and to validate the simulated water balance is still an issue, even for Switzerland, and time will be needed to establish long-term observational datasets for a robust detection of any temporal changes in these variables.

9 References

Alemohammad, S. H., Fang, B., Konings, A. G., Aires, F., Green, J. K., Kolassa, J., Miralles, D., Prigent, C. and Gentine, P.: Water, Energy, and Carbon with Artificial Neural Networks (WECANN): a statistically based estimate of global surface turbulent fluxes and gross primary productivity using solar-induced fluorescence, Biogeosciences, 14(18), 4101–4124, doi:10.5194/bg-14-4101-2017, 2017.

Alexander, L. V., Zhang, X., Peterson, T. C., Caesar, J., Gleason, B., Klein Tank, A. M. G., Haylock, M., Collins, D., Trewin, B., Rahimzadeh, F., Tagipour, A., Rupa Kumar, K., Revadekar, J., Griffiths, G., Vincent, L., Stephenson, D. B., Burn, J., Aguilar, E., Brunet, M., Taylor, M., New, M., Zhai, P., Rusticucci, M. and Vazquez-Aguirre, J. L.: Global observed

changes in daily climate extremes of temperature and precipitation, J. Geophys. Res. Atmospheres, 111(D5), D05109, doi:10.1029/2005JD006290, 2006.

Ambrose, S. M. and Sterling, S. M.: Global patterns of annual actual evapotranspiration with land-cover type: knowledge gained from a new observation-based database, Hydrol. Earth Syst. Sci. Discuss., 11, 12103–12135, doi:10.5194/hessd-11-12103-2014, 2014.

Bader, S.: Die extreme Sommerhitze im aussergewöhnlichen Witterungsjahr 2003, Arbeitsbericht, MeteoSchweiz., 2004.

BAFU: Hitze und Trockenheit im Sommer 2015. Auswirkungen auf Mensch und Umwelt., Bundesamt für Umwelt BAFU, Bern, Schweiz., 2016.

Baldocchi, D., Falge, E., Gu, L., Olson, R., Hollinger, D., Running, S., Anthoni, P., Bernhofer, Ch., Davis, K., Evans, R., Fuentes, J., Goldstein, A., Katul, G., Law, B., Lee, X., Malhi, Y., Meyers, T., Munger, W., Oechel, W., Paw U, K. T., Pilegaard, K., Schmid, H. P., Valentini, R., Verma, S., Vesala, T., Wilson, K. and Wofsy, S.: FLUXNET: A New Tool to Study the Temporal and Spatial Variability of Ecosystem-Scale Carbon Dioxide, Water Vapor, and Energy Flux Densities, Bull. Am. Meteorol. Soc., 82(11), 2415–2434, doi:10.1175/1520-0477(2001)082<2415:FANTTS>2.3.CO;2, 2001.

Balsamo, G., Albergel, C., Beljaars, A., Boussetta, S., Brun, E., Cloke, H., Dee, D., Dutra, E., Muñoz-Sabater, J., Pappenberger, F., de Rosnay, P., Stockdale, T. and Vitart, F.: ERA-Interim/Land: a global land surface reanalysis data set, Hydrol. Earth Syst. Sci., 19(1), 389–407, doi:10.5194/hess-19-389-2015, 2015.

Barriopedro, D., Fischer, E. M., Luterbacher, J., Trigo, R. M. and García-Herrera, R.: The Hot Summer of 2010: Redrawing the Temperature Record Map of Europe, Science, 1201224, doi:10.1126/science.1201224, 2011.

Bartók, B., Wild, M., Folini, D., Lüthi, D., Kotlarski, S., Schär, C., Vautard, R., Jerez, S. and Imecs, Z.: Projected changes in surface solar radiation in CMIP5 global climate models and in EURO-CORDEX regional climate models for Europe, Clim. Dyn., 49(7), 2665–2683, doi:10.1007/s00382-016-3471-2, 2017.

Berg, A., Sheffield, J. and Milly, P. C. D.: Divergent surface and total soil moisture projections under global warming, Geophys. Res. Lett., 44(1), 2016GL071921, doi:10.1002/2016GL071921, 2017.

Bernacchi, C. J. and VanLoocke, A.: Terrestrial Ecosystems in a Changing Environment: A Dominant Role for Water, Annu. Rev. Plant Biol., 66(1), 599–622, doi:10.1146/annurev-arplant-043014-114834, 2015.

Blauhut, V., Gudmundsson, L. and Stahl, K.: Towards pan-European drought risk maps: quantifying the link between drought indices and reported drought impacts, Environ. Res. Lett., 10(1), 014008, doi:10.1088/1748-9326/10/1/014008, 2015.

Boé, J. and Terray, L.: Uncertainties in summer evapotranspiration changes over Europe and implications for regional climate change, Geophys. Res. Lett., 35(L05702), doi:10.1029/2007GL032417, 2008.

Bonan, G. B.: Forests and Climate Change: Forcings, Feedbacks, and the Climate Benefits of Forests, Science, 320(5882), 1444–1449, 2008.

Brocca, L., Zucco, G., Mittelbach, H., Moramarco, T. and Seneviratne, S. I.: Absolute versus temporal anomaly and percent of saturation soil moisture spatial variability for six networks worldwide, Water Resour. Res., 50(7), 5560–5576, doi:10.1002/2014WR015684, 2014.

BUWAL, BWG and MeteoSchweiz: Auswirkungen des Hitzesommers 2003 auf die Gewässer., Bundesamt für Umwelt, Wald und Landschaft, Bern, Schweiz., 2004.

Byrne, M. P. and O'Gorman, P. A.: The Response of Precipitation Minus Evapotranspiration to Climate Warming: Why the "Wet-Get-Wetter, Dry-Get-Drier" Scaling Does Not Hold over Land, J. Clim., 28(20), 8078–8092, doi:10.1175/JCLI-D-15-0369.1, 2015.

Calanca, P.: Interannual variability of summer mean soil moisture conditions in Switzerland during the 20th century: A look using a stochastic soil moisture model, Water Resour. Res., 40(12), W12502, doi:10.1029/2004WR003254, 2004.

Calanca, P.: Climate change and drought occurrence in the Alpine region: How severe are becoming the extremes?, Glob. Planet. Change, 57(1–2), 151–160, doi:10.1016/j.gloplacha.2006.11.001, 2007.

Calanca, P. and Fuhrer, J.: Swiss Agriculture in a Changing Climate: Grassland Production and its Economic Value, in The Coupling of Climate and Economic Dynamics: Essays on Integrated Assessment, edited by A. Haurie and L. Viguier, pp. 341–353, Springer Netherlands, Dordrecht., 2005.

Calanca, P., Roesch, A., Jasper, K. and Wild, M.: Global warming and the summertime evapotranspiration regime of the Alpine region, Clim. Change, 79(1–2), 65–78, doi:10.1007/s10584-006-9103-9, 2006.

CH2011: Swiss Climate Change Scenarios CH2011, C2SM, MeteoSwiss, ETH, NCCR Climate, and OcCC, Zürich, Switzerland., 2011.

CH2018: CH2018 – Climate Scenarios for Switzerland, National Centre for Climate Services., 2018.

Chen, L., Dirmeyer, P. A., Guo, Z. and Schultz, N. M.: Pairing FLUXNET sites to validate model representations of land-use/land-cover change, Hydrol. Earth Syst. Sci., 22(1), 111–125, doi:10.5194/hess-22-111-2018, 2018.

Christensen, J. H. and Christensen, O. B.: A summary of the PRUDENCE model projections of changes in European climate by the end of this century, Clim. Change, 81(1), 7–30, doi:10.1007/s10584-006-9210-7, 2007.

Coenders-Gerrits, A. M. J., van der Ent, R. J., Bogaard, T. A., Wang-Erlandsson, L., Hrachowitz, M. and Savenije, H. H. G.: Uncertainties in transpiration estimates, Nature, 506(7487), E1–E2, doi:10.1038/nature12925, 2014.

Corti, T., Muccione, V., Köllner-Heck, P., Bresch, D. and Seneviratne, S. I.: Simulating past droughts and associated building damages in France, Hydrol. Earth Syst. Sci., 13(9), 1739–1747, doi:10.5194/hess-13-1739-2009, 2009.

Dai, A.: Drought under global warming: A review, Wiley Interdiscip. Rev. Clim. Change, 2, 45–65, doi:10.1002/wcc.81, 2011.

Dai, A., Trenberth, K. E. and Qian, T.: A Global Dataset of Palmer Drought Severity Index for 1870–2002: Relationship with Soil Moisture and Effects of Surface Warming, J. Hydrometeorol., 5(6), 1117–1130, 2004.

Davin, E. L. and Seneviratne, S. I.: Role of land surface processes and diffuse/direct radiation partitioning in simulating the European climate, Biogeosciences, 9(5), 1695–1707, doi:10.5194/bg-9-1695-2012, 2012.

Davin, E. L., Noblet-Ducoudré, N. de and Friedlingstein, P.: Impact of land cover change on surface climate: Relevance of the radiative forcing concept, Geophys. Res. Lett., 34(L13702), doi:10.1029/2007GL029678, 2007.

Davin, E. L., Stöckli, R., Jaeger, E. B., Levis, S. and Seneviratne, S. I.: COSMO-CLM^2: a new version of the COSMO-CLM model coupled to the Community Land Model, Clim. Dyn., 37(9), 1889–1907, doi:10.1007/s00382-011-1019-z, 2011.

Davin, E. L., Seneviratne, S. I., Ciais, P., Olioso, A. and Wang, T.: Preferential cooling of hot extremes from cropland albedo management, Proc. Natl. Acad. Sci., 111(27), 9757–9761, doi:10.1073/pnas.1317323111, 2014.

Davin, E. L., Maisonnave, E. and Seneviratne, S. I.: Is land surface processes representation a possible weak link in current Regional Climate Models?, Environ. Res. Lett., 11(7), 074027, doi:10.1088/1748-9326/11/7/074027, 2016.

De Boeck, H. J. and Verbeeck, H.: Drought-associated changes in climate and their relevance for ecosystem experiments and models, Biogeosciences, 8(5), 1121–1130, doi:10.5194/bg-8-1121-2011, 2011.

Donohue, R. J., Roderick, M. L., McVicar, T. R. and Farquhar, G. D.: Impact of CO_2 fertilization on maximum foliage cover across the globe's warm, arid environments, Geophys. Res. Lett., 40(12), 3031–3035, doi:10.1002/grl.50563, 2013.

Donohue, R. J., Roderick, M. L., McVicar, T. R. and Yang, Y.: A simple hypothesis of how leaf and canopy-level transpiration and assimilation respond to elevated CO_2 reveals distinct response patterns between disturbed and undisturbed vegetation, J. Geophys. Res. Biogeosciences, 122(1), 168–184, doi:10.1002/2016JG003505, 2017.

Dorigo, W., Wagner, W., Albergel, C., Albrecht, F., Balsamo, G., Brocca, L., Chung, D., Ertl, M., Forkel, M., Gruber, A., Haas, E., Hamer, P. D., Hirschi, M., Ikonen, J., Jeu, R. de, Kidd, R., Lahoz, W., Liu, Y. Y., Miralles, D., Mistelbauer, T., Nicolai-Shaw, N., Parinussa, R., Pratola, C., Reimer, C., Schalie, R. van der, Seneviratne, S. I., Smolander, T. and Lecomte, P.: ESA CCI Soil Moisture for improved Earth system understanding: State-of-the art and future directions, Remote Sens. Environ., doi:10.1016/j.rse.2017.07.001, 2017.

Duveiller, G., Hooker, J. and Cescatti, A.: The mark of vegetation change on Earth's surface energy balance, Nat. Commun., 9(1), 679, doi:10.1038/s41467-017-02810-8, 2018.

Engineer, C. B., Hashimoto-Sugimoto, M., Negi, J., Israelsson-Nordström, M., Azoulay-Shemer, T., Rappel, W.-J., Iba, K. and Schroeder, J. I.: CO_2 sensing and CO_2 regulation of stomatal conductance: advances and open questions, Trends Plant Sci., 21(1), 16–30, 2016.

Fatichi, S., Leuzinger, S., Paschalis, A., Langley, J. A., Donnellan Barraclough, A. and Hovenden, M. J.: Partitioning direct and indirect effects reveals the response of water-limited ecosystems to elevated CO_2, Proc. Natl. Acad. Sci., 113(45), 12757–12762, doi:10.1073/pnas.1605036113, 2016.

Fleig, A. K., Tallaksen, L. M., Hisdal, H. and Hannah, D. M.: Regional hydrological drought in north-western Europe: linking a new Regional Drought Area Index with weather types, Hydrol. Process., 25(7), 1163–1179, doi:10.1002/hyp.7644, 2011.

Frich, P., Alexander, L. V., Della-Marta, P., Gleason, B., Haylock, M., Tank, A. M. G. K. and Peterson, T.: Observed coherent changes in climatic extremes during the second half of the twentieth century, Clim. Res., 19(3), 193–212, 2002.

Fuhrer, J. and Jasper, K.: Bewässerungsbedürftigkeit von Acker- und Grasland im heutigen Klima, Agrarforschung, 16(10), 396–401, 2009.

Fuhrer, J., Beniston, M., Fischlin, A., Frei, Ch., Goyette, S., Jasper, K. and Pfister, Ch.: Climate Risks and Their Impact on Agriculture and Forests in Switzerland, Clim. Change, 79(1), 79–102, doi:10.1007/s10584-006-9106-6, 2006.

García-Herrera, R., Díaz, J., Trigo, R. M., Luterbacher, J. and Fischer, E. M.: A Review of the European Summer Heat Wave of 2003, Crit. Rev. Environ. Sci. Technol., 40(4), 267–306, 2010.

Giorgi, F. and Gao, X.-J.: Regional earth system modeling: review and future directions, Atmospheric Ocean. Sci. Lett., 11(2), 189–197, doi:10.1080/16742834.2018.1452520, 2018.

Greve, P. and Seneviratne, S. I.: Assessment of future changes in water availability and aridity, Geophys. Res. Lett., 42(13), 5493–5499, doi:10.1002/2015GL064127, 2015.

Greve, P., Roderick, M. L. and Seneviratne, S. I.: Simulated changes in aridity from the last glacial maximum to $4xCO_2$, Environ. Res. Lett., 12(11), 114021, doi:10.1088/1748-9326/aa89a3, 2017.

Greve, P., Gudmundsson, L. and Seneviratne, S. I.: Regional scaling of annual mean precipitation and water availability with global temperature change, Earth Syst Dynam, 9(1), 227–240, doi:10.5194/esd-9-227-2018, 2018.

Gudmundsson, L. and Seneviratne, S. I.: European drought trends, in Proceedings of the International Association of Hydrological Sciences, vol. 369, pp. 75–79, Copernicus., 2015a.

Gudmundsson, L. and Seneviratne, S. I.: Towards observation-based gridded runoff estimates for Europe, Hydrol Earth Syst Sci, 19(6), 2859–2879, doi:10.5194/hess-19-2859-2015, 2015b.

Gudmundsson, L. and Seneviratne, S. I.: Anthropogenic climate change affects meteorological drought risk in Europe, Environ. Res. Lett., 11(4), doi:10.1088/1748-9326/11/4/044005, 2016a.

Gudmundsson, L. and Seneviratne, S. I.: Observation-based gridded runoff estimates for Europe (E-RUN version 1.1), Earth Syst. Sci. Data, 8(2), 279–295, doi:10.5194/essd-8-279-2016, 2016b.

Gudmundsson, L., Rego, F. C., Rocha, M. and Seneviratne, S. I.: Predicting above normal wildfire activity in southern Europe as a function of meteorological drought, Environ. Res. Lett., 9(8), 084008, doi:10.1088/1748-9326/9/8/084008, 2014.

Gudmundsson, L., Seneviratne, S. I. and Zhang, X.: Anthropogenic climate change detected in European renewable freshwater resources, Nat. Clim. Change, 7(11), 813–816, doi:10.1038/nclimate3416, 2017.

Gutowski Jr., W. J., Giorgi, F., Timbal, B., Frigon, A., Jacob, D., Kang, H.-S., Raghavan, K., Lee, B., Lennard, C., Nikulin, G., O'Rourke, E., Rixen, M., Solman, S., Stephenson, T. and Tangang, F.: WCRP COordinated Regional Downscaling EXperiment (CORDEX): a diagnostic MIP for CMIP6, Geosci. Model Dev., 9(11), 4087–4095, doi:10.5194/gmd-9-4087-2016, 2016.

Haddeland, I., Heinke, J., Biemans, H., Eisner, S., Flörke, M., Hanasaki, N., Konzmann, M., Ludwig, F., Masaki, Y., Schewe, J., Stacke, T., Tessler, Z. D., Wada, Y. and Wisser, D.: Global water resources affected by human interventions and climate change, Proc. Natl. Acad. Sci., 111(9), 3251–3256, doi:10.1073/pnas.1222475110, 2014.

Haylock, M. R., Hofstra, N., Tank, A. M. G. K., Klok, E. J., Jones, P. D. and New, M.: A European daily high-resolution gridded data set of surface temperature and precipitation for 1950–2006, J. Geophys. Res. Atmospheres, 113(D20), doi:10.1029/2008JD010201, 2008.

Heim, R. R.: A Review of Twentieth-Century Drought Indices Used in the United States, Bull. Am. Meteorol. Soc., 83(8), 1149--1165, doi:10.1175/1520-0477(2002)083<1149:AROTDI>2.3.CO;2, 2002.

Hirschi, M., Seneviratne, S. I., Alexandrov, V., Boberg, F., Boroneant, C., Christensen, O. B., Formayer, H., Orlowsky, B. and Stepanek, P.: Observational evidence for soil-moisture impact on hot extremes in southeastern Europe, Nat. Geosci., 4(1), 17–21, doi:10.1038/ngeo1032, 2011.

Hirschi, M., Michel, D., Lehner, I. and Seneviratne, S. I.: A site-level comparison of lysimeter and eddy covariance flux measurements of evapotranspiration, Hydrol. Earth Syst. Sci., 21(3), 1809--1825, doi:10.5194/hess-21-1809-2017, 2017.

Hong, T., Dong, W., Ji, D., Dai, T., Yang, S. and Wei, T.: The response of vegetation to rising CO_2 concentrations plays an important role in future changes in the hydrological cycle, Theor. Appl. Climatol., doi:10.1007/s00704-018-2476-7, 2018.

van den Hurk, B., Doblas-Reyes, F., Balsamo, G., Koster, R., Seneviratne, S. and Camargo, H.: Soil moisture effects on seasonal temperature and precipitation forecast scores in Europe, Clim. Dyn., doi:10.1007/s00382-010-0956-2, 2010.

IPCC: Climate Change 2013: The Physical Science Basis. Contribution of Working Group I to the Fifth Assessment Report of the Intergovernmental Panel on Climate Change, edited by T. F. Stocker, D. Qin, G.-K. Plattner, M. Tignor, S. K. Allen, J. Boschung, A. Nauels, Y. Xia, V. Bex, and P. M. Midgley, Cambridge University Press, Cambridge, United Kingdom and New York, NY, USA., 2013.

Isotta, F. A., Frei, C., Weilguni, V., Tadić, M. P., Lassègues, P., Rudolf, B., Pavan, V., Cacciamani, C., Antolini, G., Ratto, S. M., Munari, M., Micheletti, S., Bonati, V., Lussana, C., Ronchi, C., Panettieri, E., Marigo, G. and Vertačnik, G.: The climate of daily precipitation in the Alps: development and analysis of a high-resolution grid dataset from pan-Alpine rain-gauge data, Int. J. Climatol., 34(5), 1657–1675, doi:10.1002/joc.3794, 2014.

Jacob, D., Petersen, J., Eggert, B., Alias, A., Christensen, O. B., Bouwer, L. M., Braun, A., Colette, A., Déqué, M., Georgievski, G., Georgopoulou, E., Gobiet, A., Menut, L., Nikulin, G., Haensler, A., Hempelmann, N., Jones, C., Keuler, K., Kovats, S., Kröner, N., Kotlarski, S., Kriegsmann, A., Martin, E., van Meijgaard, E., Moseley, C., Pfeifer, S., Preuschmann, S., Radermacher, C., Radtke, K., Rechid, D., Rounsevell, M., Samuelsson, P., Somot, S., Soussana, J.-F., Teichmann, C., Valentini, R., Vautard, R., Weber, B. and Yiou, P.: EURO-CORDEX: new high-resolution climate change projections for European impact research, Reg. Environ. Change, 14(2), 563–578, doi:10.1007/s10113-013-0499-2, 2014.

Jasechko, S., Sharp, Z. D., Gibson, J. J., Birks, S. J., Yi, Y. and Fawcett, P. J.: Terrestrial water fluxes dominated by transpiration, Nature, 496(7445), 347–350, doi:10.1038/nature11983, 2013.

Jasper, K., Calanca, P. and Fuhrer, J.: Changes in summertime soil water patterns in complex terrain due to climatic change, J. Hydrol., 327(3), 550–563, doi:10.1016/j.jhydrol.2005.11.061, 2006.

Jiménez, C., Prigent, C., Mueller, B., Seneviratne, S. I., McCabe, M. F., Wood, E. F., Rossow, W. B., Balsamo, G., Betts, A. K., Dirmeyer, P. A., Fisher, J. B., Jung, M., Kanamitsu, M., Reichle, R. H., Reichstein, M., Rodell, M., Sheffield, J., Tu, K. and Wang, K.: Global intercomparison of 12 land surface heat flux estimates, J. Geophys. Res., 116(D2), doi:10.1029/2010JD014545, 2011.

Jung, M., Reichstein, M. and Bondeau, A.: Towards global empirical upscaling of FLUXNET eddy covariance observations: validation of a model tree ensemble approach using a biosphere model, Biogeosciences, 6(10), 2001–2013, doi:10.5194/bg-6-2001-2009, 2009.

Jung, M., Reichstein, M., Ciais, P., Seneviratne, S. I., Sheffield, J., Goulden, M. L., Bonan, G., Cescatti, A., Chen, J., de Jeu, R., Dolman, A. J., Eugster, W., Gerten, D., Gianelle, D., Gobron, N., Heinke, J., Kimball, J., Law, B. E., Montagnani, L., Mu, Q., Mueller, B., Oleson, K., Papale, D., Richardson, A. D., Roupsard, O., Running, S., Tomelleri, E., Viovy, N., Weber, U., Williams, C., Wood, E., Zaehle, S. and Zhang, K.: Recent decline in the global land evapotranspiration trend due to limited moisture supply, Nature, 467(7318), 951–954, 2010.

Keenan, T. F., Hollinger, D. Y., Bohrer, G., Dragoni, D., Munger, J. W., Schmid, H. P. and Richardson, A. D.: Increase in forest water-use efficiency as atmospheric carbon dioxide concentrations rise, Nature, 499(7458), 324, 2013.

Keller, F. and Fuhrer, J.: Die Landwirtschaft und der Hitzesommer 2003, Agrar. Schweiz, 11(9), 403–410, 2004.

Kjellström, E., Nikulin, G., Strandberg, G., Christensen, O. B., Jacob, D., Keuler, K., Lenderink, G., Meijgaard, E. van, Schär, C., Somot, S., Sørland, S. L., Teichmann, C. and Vautard, R.: European climate change at global mean temperature increases of 1.5 and 2 °C above pre-industrial conditions as simulated by the EURO-CORDEX regional climate models, Earth Syst. Dyn., 9(2), 459–478, doi:10.5194/esd-9-459-2018, 2018.

Koster, R. D. and Suarez, M. J.: Soil moisture memory in climate models, J. Hydrometeorol., 21, 558–570, 2001.

Koster, R. D., Schubert, S. D. and Suarez, M. J.: Analyzing the Concurrence of Meteorological Droughts and Warm Periods, with Implications for the Determination of Evaporative Regime, J. Clim., 22(12), 3331–3341, 2009.

Koster, R. D., Mahanama, S. P. P., Yamada, T. J., Balsamo, G., Berg, A. A., Boisserie, M., Dirmeyer, P. A., Doblas-Reyes, F. J., Drewitt, G., Gordon, C. T., Guo, Z., Jeong, J.-H., Lawrence, D. M., Lee, W.-S., Li, Z., Luo, L., Malyshev, S., Merryfield, W. J., Seneviratne, S. I., Stanelle, T., van den Hurk, B. J. J. M., Vitart, F. and Wood, E. F.: Contribution of land surface initialization to subseasonal forecast skill: First results from a multi-model experiment, Geophys. Res. Lett., 37(L02402), doi:10.1029/2009GL041677, 2010.

Lemordant, L. and Gentine, P.: Vegetation Response to Rising CO_2 Impacts Extreme Temperatures, Geophys. Res. Lett., 46(3), 1383–1392, doi:10.1029/2018GL080238, 2019.

Lemordant, L., Gentine, P., Swann, A. S., Cook, B. I. and Scheff, J.: Critical impact of vegetation physiology on the continental hydrologic cycle in response to increasing CO_2, Proc. Natl. Acad. Sci., 115(16), 4093–4098, doi:10.1073/pnas.1720712115, 2018.

Liu, Y. Y., Dorigo, W. A., Parinussa, R. M., Jeu, R. A. M. de, Wagner, W., McCabe, M. F., Evans, J. P. and Dijk, A. I. J. M. van: Trend-preserving blending of passive and active microwave soil moisture retrievals, Remote Sens. Environ., 123(0), 280–297, doi:10.1016/j.rse.2012.03.014, 2012.

Lloyd-Hughes, B. and Saunders, M. A.: A drought climatology for Europe, Int J. Climatol., 22(13), 1571–1592, 2002.

Martens, B., Miralles, D. G., Lievens, H., Schalie, R. van der, Jeu, R. A. M. de, Fernández-Prieto, D., Beck, H. E., Dorigo, W. A. and Verhoest, N. E. C.: GLEAM v3: satellite-based land evaporation and root-zone soil moisture, Geosci. Model Dev., 10(5), 1903–1925, doi:10.5194/gmd-10-1903-2017, 2017.

McGrath, M. J., Luyssaert, S., Meyfroidt, P., Kaplan, J. O., Bürgi, M., Chen, Y., Erb, K., Gimmi, U., McInerney, D., Naudts, K., Otto, J., Pasztor, F., Ryder, J., Schelhaas, M.-J. and Valade, A.: Reconstructing European forest management from 1600 to 2010, Biogeosciences, 12(14), 4291–4316, doi:10.5194/bg-12-4291-2015, 2015.

McKee, T. B., Doesken, N. J. and Kleist, J.: The relationship of drought frequency and duration to time scales, Eighth Conference on Applied Climatology, Anaheim, California, USA., 1993.

Meier, R., Davin, E. L., Lejeune, Q., Hauser, M., Li, Y., Martens, B., Schultz, N. M., Sterling, S. and Thiery, W.: Evaluating and improving the Community Land Model's sensitivity to land cover, Biogeosciences, 15(15), 4731–4757, doi:10.5194/bg-15-4731-2018, 2018.

MeteoSchweiz: Der Hitzesommer 2015 in der Schweiz, Fachbericht MeteoSchweiz, MeteoSchweiz., 2016.

MeteoSchweiz: Hitze und Trockenheit im Sommerhalbjahr 2018 – eine klimatologische Übersicht, Fachbericht MeteoSchweiz., 2018.

Michel, D., Jiménez, C., Miralles, D. G., Jung, M., Hirschi, M., Ershadi, A., Martens, B., McCabe, M. F., Fisher, J. B., Mu, Q., Seneviratne, S. I., Wood, E. F. and Fernández-Prieto, D.: The WACMOS-ET project – Part 1: Tower-scale evaluation of four remote-sensing-based evapotranspiration algorithms, Hydrol Earth Syst Sci, 20(2), 803–822, doi:10.5194/hess-20-803-2016, 2016.

Milly, P. C. D. and Dunne, K. A.: Potential evapotranspiration and continental drying, Nat. Clim. Change, 6(10), 946–949, doi:10.1038/nclimate3046, 2016.

Milly, P. C. D. and Dunne, K. A.: A Hydrologic Drying Bias in Water-Resource Impact Analyses of Anthropogenic Climate Change, JAWRA J. Am. Water Resour. Assoc., 53(4), 822–838, doi:10.1111/1752-1688.12538, 2017.

Miralles, D. G., De Jeu, R. A. M., Gash, J. H., Holmes, T. R. H. and Dolman, A. J.: Magnitude and variability of land evaporation and its components at the global scale, Hydrol. Earth Syst. Sci., 15(3), 967–981, doi:10.5194/hess-15-967-2011, 2011.

Miralles, D. G., van den Berg, M. J., Gash, J. H., Parinussa, R. M., de Jeu, R. A. M., Beck, H. E., Holmes, T. R. H., Jiménez, C., Verhoest, N. E. C., Dorigo, W. A., Teuling, A. J. and Johannes Dolman, A.: El Niño–La Niña cycle and recent trends in continental evaporation, Nat. Clim. Change, 4, 122–126, doi:10.1038/nclimate2068, 2014a.

Miralles, D. G., Teuling, A. J., van Heerwaarden, C. C. and Vila-Guerau de Arellano, J.: Mega-heatwave temperatures due to combined soil desiccation and atmospheric heat accumulation, Nat. Geosci., 7, 345–349, doi:10.1038/ngeo2141, 2014b.

Miralles, D. G., Jiménez, C., Jung, M., Michel, D., Ershadi, A., McCabe, M. F., Hirschi, M., Martens, B., Dolman, A. J., Fisher, J. B., Mu, Q., Seneviratne, S. I., Wood, E. F. and Fernández-Prieto, D.: The WACMOS-ET project – Part 2: Evaluation of global terrestrial evaporation data sets, Hydrol Earth Syst Sci, 20(2), 823–842, doi:10.5194/hess-20-823-2016, 2016.

Mittelbach, H.: Soil Moisture in Switzerland: Analyses from the Swiss Soil Moisture Experiment, PhD Thesis, ETH Zürich, Zürich, Switzerland., 2011.

Mittelbach, H. and Seneviratne, S. I.: A new perspective on the spatio-temporal variability of soil moisture: temporal dynamics versus time-invariant contributions, Hydrol. Earth Syst. Sci., 16(7), 2169–2179, doi:10.5194/hess-16-2169-2012, 2012.

Morison, J. I. L.: Sensitivity of stomata and water use efficiency to high CO_2, Plant Cell Environ., 8(6), 467–474, doi:10.1111/j.1365-3040.1985.tb01682.x, 1985.

Mueller, B. and Seneviratne, S. I.: Hot days induced by precipitation deficits at the global scale, Proc. Natl. Acad. Sci., 109(31), 12398–12403, doi:10.1073/pnas.1204330109, 2012.

Mueller, B. and Seneviratne, S. I.: Systematic land climate and evapotranspiration biases in CMIP5 simulations, Geophys. Res. Lett., 41, 128–134, doi:10.1002/2013GL058055, 2014.

Mueller, B., Hirschi, M., Jimenez, C., Ciais, P., Dirmeyer, P. A., Dolman, A. J., Fisher, J. B., Jung, M., Ludwig, F., Maignan, F., Miralles, D. G., McCabe, M. F., Reichstein, M., Sheffield, J., Wang, K., Wood, E. F., Zhang, Y. and Seneviratne, S. I.: Benchmark products for land evapotranspiration: LandFlux-EVAL multi-data set synthesis, Hydrol. Earth Syst. Sci., 17(10), 3707–3720, doi:10.5194/hess-17-3707-2013, 2013.

Nabat, P., Kiki, Somot, S., Mallet, M. and Michou, M.: Impact of Aerosols in Regional Climate Projections Over the Mediterranean Area, in Air Pollution Modeling and its Application XXIV, edited by D. G. Steyn and N. Chaumerliac, pp. 73–78, Springer International Publishing, Cham., 2016.

Naudts, K., Chen, Y., McGrath, M. J., Ryder, J., Valade, A., Otto, J. and Luyssaert, S.: Europe's forest management did not mitigate climate warming, Science, 351(6273), 597–600, doi:10.1126/science.aad7270, 2016.

Nicolai-Shaw, N., Gudmundsson, L., Hirschi, M. and Seneviratne, S. I.: Long-term predictability of soil moisture dynamics at the global scale: Persistence versus large-scale drivers, Geophys. Res. Lett., 43, 8554–8562, doi:10.1002/2016GL069847, 2016.

Nicolai-Shaw, N., Zscheischler, J., Hirschi, M., Gudmundsson, L. and Seneviratne, S. I.: A drought event composite analysis using satellite remote-sensing based soil moisture, Remote Sens. Environ., doi:10.1016/j.rse.2017.06.014, 2017.

Oleson, K. W., Lawrence, D. M., B, G., Flanner, M. G., Kluzek, E., J, P., Levis, S., Swenson, S. C., Thornton, E., Feddema, J., Heald, C. L., Jean-francois Lamarque, Niu, G., Qian, T., Running, S., Koichi Sakaguchi, Yang, L., Zeng, X., Zeng, X. and Mark Decker: Technical Description of version 4.0 of the Community Land Model (CLM), NCAR., 2010.

Orlowsky, B. and Seneviratne, S. I.: Elusive drought: uncertainty in observed trends and short- and long-term CMIP5 projections, Hydrol. Earth Syst. Sci., 17(5), 1765–1781, doi:10.5194/hess-17-1765-2013, 2013.

Orth, R. and Seneviratne, S. I.: Analysis of soil moisture memory from observations in Europe, J. Geophys. Res., 117(D15), D15115, doi:10.1029/2011JD017366, 2012.

Orth, R. and Seneviratne, S. I.: Introduction of a simple-model-based land surface dataset for Europe, Environ. Res. Lett., 10(4), doi:10.1088/1748-9326/10/4/044012, 2015.

Orth, R., Zscheischler, J. and Seneviratne, S. I.: Record dry summer in 2015 challenges precipitation projections in Central Europe, Sci. Rep., 6, doi:10.1038/srep28334, 2016.

Padrón, R. S., Gudmundsson, L. and Seneviratne, S. I.: Observational Constraints Reduce Likelihood of Extreme Changes in Multidecadal Land Water Availability, Geophys. Res. Lett., 46(2), 736–744, doi:10.1029/2018GL080521, 2019.

Pellet, C. and Hauck, C.: Monitoring soil moisture from middle to high elevation in Switzerland: set-up and first results from the SOMOMOUNT network, Hydrol. Earth Syst. Sci., 21(6), 3199--3220, doi:10.5194/hess-21-3199-2017, 2017.

Perkins, S. E.: A review on the scientific understanding of heatwaves—Their measurement, driving mechanisms, and changes at the global scale, Atmospheric Res., 164–165, 242–267, doi:10.1016/j.atmosres.2015.05.014, 2015.

Pfister, C.: Wetternachhersage, Verlag Paul Haupt, Bern., 1999.

Pfister, C. and Rutishauser, T.: Dürresommer im Schweizer Mittelland seit 1525, Unterlagen zum OcCC/ProClim- Workshop vom 4. April 2000 in Bern, OcCC. [online] Available from: http://www.occc.ch/pdf/1350.pdf, 2000.

ProClim: Hitzesommer 2003. Synthesebericht, ProClim, Bern, Switzerland. [online] Available from: http://www.proclim.ch/4dcgi/occc/de/Report?137, 2005.

Quesada, B., Vautard, R., Yiou, P., Hirschi, M. and Seneviratne, S. I.: Asymmetric European summer heat predictability from wet and dry southern winters and springs, Nat. Clim. Change, 2(10), 736–741, doi:10.1038/nclimate1536, 2012.

Rana, G. and Katerji, N.: Measurement and estimation of actual evapotranspiration in the field under Mediterranean climate: A review, Eur. J. Agron., 13(2), 125–153, doi:10.1016/S1161-0301(00)00070-8, 2000.

Renaud, V., Innes, J. L., Dobbertin, M. and Rebetez, M.: Comparison between open-site and below-canopy climatic conditions in Switzerland for different types of forests over 10 years (1998–2007), Theor. Appl. Climatol., 105(1–2), 119–127, doi:10.1007/s00704-010-0361-0, 2011.

Reyes-Fox, M., Steltzer, H., Trlica, M., McMaster, G. S., Andales, A. A., LeCain, D. R. and Morgan, J. A.: Elevated CO_2 further lengthens growing season under warming conditions, Nature, 510(7504), 259, doi:10.1038/nature13207, 2014.

Riahi, K., Rao, S., Krey, V., Cho, C., Chirkov, V., Fischer, G., Kindermann, G., Nakicenovic, N. and Rafaj, P.: RCP 8.5–A scenario of comparatively high greenhouse gas emissions, Clim. Change, 109(1–2), 33–57, doi:10.1007/s10584-011-0149-y, 2011.

Schlesinger, W. H. and Jasechko, S.: Transpiration in the global water cycle, Agric. For. Meteorol., 189–190(0), 115–117, doi:10.1016/j.agrformet.2014.01.011, 2014.

Schmugge, T. J., Kustas, W. P., Ritchie, J. C., Jackson, T. J. and Rango, A.: Remote sensing in hydrology, Adv. Water Resour., 25(8), 1367–1385, doi:10.1016/S0309-1708(02)00065-9, 2002.

Schneider, N., Eugster, W. and Schichler, B.: The Impact of Historical Land-Use Changes on the Near-Surface Atmospheric Conditions on the Swiss Plateau, Earth Interact., 8(12), 1–27, doi:10.1175/1087-3562(2004)008<0001:TIOHLC>2.0.CO;2, 2004.

Schorer, M.: Extreme Trockensommer in der Schweiz und ihre Folgen für Natur und Wirtschaft, Geographica Bernensia G 40, Institute of Geography, University of Bern, Bern., 1992.

van der Schrier, G., Briffa, K. R., Jones, P. D. and Osborn, T. J.: Summer Moisture Variability across Europe, J. Clim., 19(12), 2818–2834, doi:10.1175/JCLI3734.1, 2006.

Schwingshackl, C., Hirschi, M. and Seneviratne, S. I.: Quantifying Spatiotemporal Variations of Soil Moisture Control on Surface Energy Balance and Near-Surface Air Temperature, J. Clim., 30(18), 7105–7124, doi:10.1175/JCLI-D-16-0727.1, 2017.

Schwingshackl, C., Davin, E. L., Hirschi, M., Sørland, S. L., Wartenburger, R. and Seneviratne, S. I.: Regional climate model projections underestimate future warming due to missing plant physiological CO_2 response, Environ. Res. Lett., 14(11), doi:10.1088/1748-9326/ab4949, 2019.

Seiz, G. and Foppa, N.: National Climate Observing System (GCOS Switzerland), MeteoSwiss and ProClim. [online] Available from: www.meteoswiss.admin.ch/home/research-and-cooperation/international-cooperation/gcos/national-climate-observation/inventory.html, 2007.

Seneviratne, S. I.: Climate science: Historical drought trends revisited, Nature, 491(7424), 338–339, 2012.

Seneviratne, S. I. and Koster, R. D.: A Revised Framework for Analyzing Soil Moisture Memory in Climate Data: Derivation and Interpretation, J. Hydrometeorol., 13(1), 404–412, doi:10.1175/JHM-D-11-044.1, 2012.

Seneviratne, S. I., Lüthi, D., Litschi, M. and Schär, C.: Land-atmosphere coupling and climate change in Europe, Nature, 443(7108), 205–209, doi:10.1038/nature05095, 2006a.

Seneviratne, S. I., Koster, R. D., Guo, Z., Dirmeyer, P. A., Kowalczyk, E., Lawrence, D., Liu, P., Lu, C. H., Mocko, D., Oleson, K. W. and Verseghy, D.: Soil Moisture Memory in AGCM Simulations: Analysis of Global Land-Atmosphere Coupling Experiment (GLACE) Data, J. Hydrometeorol., 7(5), 1090–1112, 2006b.

Seneviratne, S. I., Corti, T., Davin, E. L., Hirschi, M., Jaeger, E. B., Lehner, I., Orlowsky, B. and Teuling, A. J.: Investigating soil moisture-climate interactions in a changing climate: A review, Earth-Sci. Rev., 99(3–4), 125–161, doi:10.1016/j.earscirev.2010.02.004, 2010.

Seneviratne, S. I., Nicholls, N., Easterling, D., Goodess, C. M., Kanae, S., Kossin, J., Luo, Y., Marengo, J., McInnes, K., Rahimi, M., Reichstein, M., Sorteberg, A., Vera, C. and Zhang, X.: Changes in climate extremes and their impacts on the natural physical environment, in Managing the Risks of Extreme Events and Disasters to Advance Climate Change Adaptation, edited by C. B. Field, V. Barros, T. F. Stocker, D. Qin, D. J. Dokken, K. L. Ebi, M. D. Mastrandrea, K. J. Mach, G.-K. Plattner, S. K. Allen, M. Tignor, and P. M. Midgley, pp. 109–230, Cambridge University Press, Cambridge, United Kingdom and New York, NY, USA. [online] Available from: http://ipcc-wg2.gov/SREX/, 2012a.

Seneviratne, S. I., Lehner, I., Gurtz, J., Teuling, A. J., Lang, H., Moser, U., Grebner, D., Menzel, L., Schroff, K., Vitvar, T. and Zappa, M.: Swiss prealpine Rietholzbach research catchment and lysimeter: 32 year time series and 2003 drought event, Water Resour. Res., 48(6), W06526, doi:10.1029/2011WR011749, 2012b.

Seneviratne, S. I., Wilhelm, M., Stanelle, T., van den Hurk, B., Hagemann, S., Berg, A., Cheruy, F., Higgins, M. E., Meier, A., Brovkin, V., Claussen, M., Ducharne, A., Dufresne, J.-L., Findell, K. L., Ghattas, J., Lawrence, D. M., Malyshev, S., Rummukainen, M. and Smith, B.: Impact of soil moisture-climate feedbacks on CMIP5 projections: First results from the GLACE-CMIP5 experiment, Geophys. Res. Lett., 40(19), 5212–5217, doi:10.1002/grl.50956, 2013.

Seneviratne, S. I., Donat, M. G., Pitman, A. J., Knutti, R. and Wilby, R. L.: Allowable CO_2 emissions based on regional and impact-related climate targets, Nature, 529, 477–483, doi:10.1038/nature16542, 2016.

Seneviratne, S. I., Phipps, S. J., Pitman, A. J., Hirsch, A. L., Davin, E. L., Donat, M. G., Hirschi, M., Lenton, A., Wilhelm, M. and Kravitz, B.: Land radiative management as contributor to regional-scale climate adaptation and mitigation, Nat. Geosci., 11(2), 88–96, doi:10.1038/s41561-017-0057-5, 2018.

Sheffield, J. and Wood, E. F.: Projected changes in drought occurrence under future global warming from multi-model, multi-scenario, IPCC AR4 simulations, Clim. Dyn., 31(1), 79–105, doi:10.1007/s00382-007-0340-z, 2008.

Skinner, C. B., Poulsen, C. J. and Mankin, J. S.: Amplification of heat extremes by plant CO_2 physiological forcing, Nat. Commun., 9(1), 1094, doi:10.1038/s41467-018-03472-w, 2018.

Sørland, S. L., Schär, C., Lüthi, D. and Kjellström, E.: Bias patterns and climate change signals in GCM-RCM model chains, Environ. Res. Lett., 13(7), 074017, doi:10.1088/1748-9326/aacc77, 2018.

Stahl, K., Hisdal, H., Hannaford, J., Tallaksen, L. M., Lanen, H. A. J. van, Sauquet, E., Demuth, S., Fendekova, M. and Jódar, J.: Streamflow trends in Europe: evidence from a dataset of near-natural catchments, Hydrol. Earth Syst. Sci., 14(12), 2367–2382, doi:10.5194/hess-14-2367-2010, 2010.

Stahl, K., Kohn, I., Blauhut, V., Urquijo, J., De Stefano, L., Acácio, V., Dias, S., Stagge, J. H., Tallaksen, L. M., Kampragou, E., Van Loon, A. F., Barker, L. J., Melsen, L. A., Bifulco, C., Musolino, D., de Carli, A., Massarutto, A., Assimacopoulos, D. and Van Lanen, H. A. J.: Impacts of European drought events: insights from an international database of text-based reports, Nat Hazards Earth Syst Sci, 16(3), 801–819, doi:10.5194/nhess-16-801-2016, 2016.

Staudinger, M., Stahl, K. and Seibert, J.: A drought index accounting for snow, Water Resour. Res., 50(10), 7861–7872, doi:10.1002/2013WR015143, 2014.

Stegehuis, AnnemiekI., Vautard, R., Ciais, P., Teuling, AdriaanJ., Jung, M. and Yiou, P.: Summer temperatures in Europe and land heat fluxes in observation-based data and regional climate model simulations, Clim. Dyn., 41(2), 455–477, doi:10.1007/s00382-012-1559-x, 2013.

Swann, A. L. S., Hoffman, F. M., Koven, C. D. and Randerson, J. T.: Plant responses to increasing CO_2 reduce estimates of climate impacts on drought severity, Proc. Natl. Acad. Sci., 113(36), 10019–10024, doi:10.1073/pnas.1604581113, 2016.

Tallaksen, L. M., Stagge, J. H., Stahl, K., Gudmundsson, L., Orth, R., Seneviratne, S., Van Loon, A. and Van Lanen, H.: Characteristics and drivers of drought in Europe - a summary of the DROUGHT-R&SPI project, in Drought: Research and Science-Policy Interfacing, pp. 15–21, CRC Press., 2015.

Tebaldi, C., Hayhoe, K., Arblaster, J. M. and Meehl, G. A.: Going to the Extremes, Clim. Change, 79(3–4), 185–211, doi:10.1007/s10584-006-9051-4, 2006.

Teuling, A. J., Hirschi, M., Ohmura, A., Wild, M., Reichstein, M., Ciais, P., Buchmann, N., Ammann, C., Montagnani, L., Richardson, A. D., Wohlfahrt, G. and Seneviratne, S. I.: A regional perspective on trends in continental evaporation, Geophys. Res. Lett., 36(L02404), doi:10.1029/2008GL036584, 2009.

Teuling, A. J., Seneviratne, S. I., Stockli, R., Reichstein, M., Moors, E., Ciais, P., Luyssaert, S., van den Hurk, B., Ammann, C., Bernhofer, C., Dellwik, E., Gianelle, D., Gielen, B., Grunwald, T., Klumpp, K., Montagnani, L., Moureaux, C., Sottocornola, M. and Wohlfahrt, G.: Contrasting response of European forest and grassland energy exchange to heatwaves, Nat. Geosci, 3(10), 722–727, 2010.

Teuling, A. J., Van Loon, A. F., Seneviratne, S. I., Lehner, I., Aubinet, M., Heinesch, B., Bernhofer, C., Grünwald, T., Prasse, H. and Spank, U.: Evapotranspiration amplifies European summer drought, Geophys. Res. Lett., 40(10), 2071–2075, doi:10.1002/grl.50495, 2013.

Thiery, W., Davin, E. L., Lawrence, D. M., Hirsch, A. L., Hauser, M. and Seneviratne, S. I.: Present-day irrigation mitigates heat extremes, J. Geophys. Res., 122(3), 1403–1422, doi:10.1002/2016JD025740, 2017.

Ukkola, A. M., Prentice, I. C., Keenan, T. F., van Dijk, A. I., Viney, N. R., Myneni, R. B. and Bi, J.: Reduced streamflow in water-stressed climates consistent with CO_2 effects on vegetation, Nat. Clim. Change, 6(1), 75, 2016.

Van Lanen, H. A. J., Wanders, N., Tallaksen, L. M. and Van Loon, A. F.: Hydrological drought across the world: impact of climate and physical catchment structure, Hydrol Earth Syst Sci, 17(5), 1715–1732, doi:10.5194/hess-17-1715-2013, 2013.

Van Loon, A. F.: Hydrological drought explained, Wiley Interdiscip. Rev. Water, 2(4), 359–392, doi:10.1002/wat2.1085, 2015.

Van Loon, A. F., Ploum, S. W., Parajka, J., Fleig, A. K., Garnier, E., Laaha, G. and Van Lanen, H. A. J.: Hydrological drought types in cold climates: quantitative analysis of causing factors and qualitative survey of impacts, Hydrol Earth Syst Sci, 19(4), 1993–2016, doi:10.5194/hess-19-1993-2015, 2015.

Vanden Broucke, S., Luyssaert, S., Davin, E. L., Janssens, I. and van Lipzig, N.: New insights in the capability of climate models to simulate the impact of LUC based on temperature decomposition of paired site observations, J. Geophys. Res., 120(11), doi:10.1002/2015JD023095, 2015.

Vautard, R., Yiou, P., D'Andrea, F., Noblet, N. de, Viovy, N., Cassou, C., Polcher, J., Ciais, P., Kageyama, M. and Fan, Y.: Summertime European heat and drought waves induced by wintertime Mediterranean rainfall deficit, Geophys. Res. Lett., 34(7), L07711, doi:10.1029/2006GL028001, 2007.

Vogel, M. M., Orth, R., Cheruy, F., Hagemann, S., Lorenz, R., van den Hurk, B. J. J. M. and Seneviratne, S. I.: Regional amplification of projected changes in extreme temperatures strongly controlled by soil moisture-temperature feedbacks, Geophys. Res. Lett., 44(3), 1511–1519, doi:10.1002/2016GL071235, 2017.

Vogel, M. M., Zscheischler, J. and Seneviratne, S. I.: Varying soil moisture–atmosphere feedbacks explain divergent temperature extremes and precipitation projections in central Europe, Earth Syst. Dyn., 9(3), 1107–1125, doi:10.5194/esd-9-1107-2018, 2018.

Wartenburger, R., Hirschi, M., Donat, M. G., Greve, P., Pitman, A. J. and Seneviratne, S. I.: Changes in regional climate extremes as a function of global mean temperature: an interactive plotting framework, Geosci. Model Dev., 10(9), 3609–3634, doi:10.5194/gmd-10-3609-2017, 2017.

Westervelt, D. M., Horowitz, L. W., Naik, V., Golaz, J.-C. and Mauzerall, D. L.: Radiative forcing and climate response to projected 21st century aerosol decreases, Atmospheric Chem. Phys., 15(22), 12681–12703, doi:10.5194/acp-15-12681-2015, 2015.

Whan, K., Zscheischler, J., Orth, R., Shongwe, M., Rahimi, M., Asare, E. O. and Seneviratne, S. I.: Impact of soil moisture on extreme maximum temperatures in Europe, Weather Clim. Extrem., 9, 57–67, doi:10.1016/j.wace.2015.05.001, 2015.

Wild, M., Gilgen, H., Roesch, A., Ohmura, A., Long, C. N., Dutton, E. G., Forgan, B., Kallis, A., Russak, V. and Tsvetkov, A.: From dimmming to Brightening: Decadal changes in solar radiation at earth's surface, Science, 308(5723), 847–850, 2005.

Wild, M., Trüssel, B., Ohmura, A., Long, C. N., König-Langlo, G., Dutton, E. G. and Tsvetkov, A.: Global dimming and brightening: An update beyond 2000, J. Geophys. Res., 114(D00D13), doi:10.1029/2008JD011382, 2009.

Williams, C. A., Reichstein, M., Buchmann, N., Baldocchi, D., Beer, C., Schwalm, C., Wohlfahrt, G., Hasler, N., Bernhofer, C., Foken, T., Papale, D., Schymanski, S. and Schaefer, K.: Climate and vegetation controls on the surface water balance: Synthesis of evapotranspiration measured across a global network of flux towers, Water Resour. Res., 48(6), doi:10.1029/2011WR011586, 2012.

Wolf, S., Eugster, W., Ammann, C., Häni, M., Zielis, S., Hiller, R., Stieger, J., Imer, D., Merbold, L. and Buchmann, N.: Contrasting response of grassland versus forest carbon and water fluxes to spring drought in Switzerland, Environ. Res. Lett., 8(3), doi:10.1088/1748-9326/8/3/035007, 2013.

Zampieri, M., D'Andrea, F., Vautard, R., Ciais, P., Noblet-Ducoudré, N. de and Yiou, P.: Hot European Summers and the Role of Soil Moisture in the Propagation of Mediterranean Drought, J. Clim., 22(18), 4747–4758, 2009.

Zhang, L., Dawes, W. R. and Walker, G. R.: Response of mean annual evapotranspiration to vegetation changes at catchment scale, Water Resour. Res., 37(3), 701–708, doi:10.1029/2000WR900325, 2001.

Zscheischler, J., Orth, R. and Seneviratne, S. I.: Bivariate return periods of temperature and precipitation explain a large fraction of European crop yields, Biogeosciences, 14(13), 3309–3320, doi:10.5194/bg-14-3309-2017, 2017.